Charged-particle nuclear modification factors in XeXe collisions at $\sqrt{s_{\mathrm{NN}}} = 5.44\,\mathrm{TeV}$

The CMS collaboration

E-mail: cms-publication-committee-chair@cern.ch

ABSTRACT: The differential yields of charged particles having pseudorapidity within $|\eta| < 1$ are measured using xenon-xenon (XeXe) collisions at $\sqrt{s_{\mathrm{NN}}} = 5.44\,\mathrm{TeV}$. The data, corresponding to an integrated luminosity of $3.42\,\mu\mathrm{b}^{-1}$, were collected in 2017 by the CMS experiment at the LHC. The yields are reported as functions of collision centrality and transverse momentum, p_{T}, from 0.5 to 100 GeV. A previously reported p_{T} spectrum from proton-proton collisions at $\sqrt{s} = 5.02\,\mathrm{TeV}$ is used for comparison after correcting for the difference in center-of-mass energy. The nuclear modification factors using this reference, R_{AA}^{*}, are constructed and compared to previous measurements and theoretical predictions. In head-on collisions, the R_{AA}^{*} has a value of 0.17 in the p_{T} range of 6–8 GeV, but increases to approximately 0.7 at 100 GeV. Above $\approx 6\,\mathrm{GeV}$, the XeXe data show a notably smaller suppression than previous results for lead-lead (PbPb) collisions at $\sqrt{s_{\mathrm{NN}}} = 5.02\,\mathrm{TeV}$ when compared at the same centrality (i.e., the same fraction of total cross section). However, the XeXe suppression is slightly greater than that for PbPb in events having a similar number of participating nucleons.

Contents

1 Introduction

The transverse momentum (p_T) spectrum of charged particles is a well-studied observable for examining the hot, dense quark-gluon plasma (QGP) created in high-energy heavy ion collisions. As scattered partons traverse this medium, they experience a loss of energy due to quantum chromodynamics processes such as gluon emission and parton splitting [1]. Because high-p_T charged particles are produced through parton fragmentation and subsequent hadronization, their yields are sensitive to the strength of QGP-induced energy loss [2, 3]. In contrast, production of charged particles having p_T less than a few GeV is particularly sensitive to initial parton densities and hydrodynamic expansion of the medium [4–7].

Modification of charged-particle yields can be quantified by forming a ratio of the spectra in nucleus-nucleus (AA) and pp collisions, where the latter are multiplied by the average number of binary nucleon-nucleon collisions per AA event, $\langle N_{\mathrm{coll}} \rangle$. This observable is known as the nuclear modification factor, R_{AA}, and is given by

$$R_{\mathrm{AA}}(p_T) = \frac{1}{\langle N_{\mathrm{coll}} \rangle} \frac{\mathrm{d}N^{\mathrm{AA}}/\mathrm{d}p_T}{\mathrm{d}N^{\mathrm{pp}}/\mathrm{d}p_T}. \tag{1.1}$$

Here $\mathrm{d}N^{\mathrm{AA}}/\mathrm{d}p_T$ ($\mathrm{d}N^{\mathrm{pp}}/\mathrm{d}p_T$) is the charged-particle yield in AA (pp) collisions. An equivalent definition replaces $\mathrm{d}N^{\mathrm{pp}}/\mathrm{d}p_T$ with the differential charged-particle cross section in inelastic pp collisions, $\mathrm{d}\sigma^{\mathrm{pp}}/\mathrm{d}p_T$, and $\langle N_{\mathrm{coll}} \rangle$ with the nuclear overlap function, $T_{\mathrm{AA}} = \langle N_{\mathrm{coll}} \rangle / \sigma^{\mathrm{pp}}$:

$$R_{\mathrm{AA}}(p_T) = \frac{1}{T_{\mathrm{AA}}} \frac{\mathrm{d}N^{\mathrm{AA}}/\mathrm{d}p_T}{\mathrm{d}\sigma^{\mathrm{pp}}/\mathrm{d}p_T}. \tag{1.2}$$

Both $\langle N_{\mathrm{coll}} \rangle$ and T_{AA} can be obtained using a Glauber model of nuclear collisions [8].

Charged-particle p_T spectra and their associated nuclear modification have been explored at the BNL RHIC [9–12] in gold-gold collisions at a center-of-mass energy per nucleon pair ($\sqrt{s_{\mathrm{NN}}}$) of up to 200 GeV. These analyses found R_{AA} to be strongly suppressed in head-on collisions, with minima around $p_T = 5\,\mathrm{GeV}$. Measurements made at the CERN LHC by the ALICE [13, 14], ATLAS [15], and CMS [16, 17] Collaborations have explored the same observables in lead-lead (PbPb) collisions at $\sqrt{s_{\mathrm{NN}}} = 2.76$ and 5.02 TeV. These studies found minima of R_{AA} around 0.15 at $p_T = 8\,\mathrm{GeV}$. They also indicate that R_{AA} increases to values around 0.7 at $p_T = 100\,\mathrm{GeV}$. Complementary measurements of the nuclear modification factor in proton-lead (pPb) collisions at $\sqrt{s_{\mathrm{NN}}} = 5.02\,\mathrm{TeV}$ indicate that high-p_T charged-particle yields are not strongly modified in this smaller colliding system, ruling out effects related to the initial-state conditions of the lead nucleus as a cause of the high-p_T suppression seen in PbPb collisions [14, 17, 18]. Together, these observations indicate strong p_T-dependent energy loss due to the presence of the QGP in heavy ion collisions.

In 2017, the LHC collided ^{129}Xe nuclei at $\sqrt{s_{\mathrm{NN}}} = 5.44\,\mathrm{TeV}$. The LHC had previously only provided proton-proton (pp), pPb, and PbPb collisions. Therefore, the xenon-xenon (XeXe) data provide a unique opportunity to explore the properties of the QGP using an intermediate size collision system at LHC energies. Xenon collisions also provide an opportunity to test the system size dependence of parton energy loss. The radii of xenon and lead nuclei are $\approx$5.4 and $\approx$6.6 fm, respectively [19]. Assuming the energy loss of a parton is linearly (quadratically) related to only its path length through the QGP would imply an average reduction in energy loss of 17 (31)% in head-on XeXe collisions as compared to PbPb collisions. This difference could manifest itself in comparisons of the charged-particle spectra between the two systems. Recent results from the ALICE Collaboration indicate this is the case, with the R_{AA} of head-on XeXe collisions being less suppressed than that of PbPb collisions [20]. Comparisons of copper-copper and gold-gold collisions at RHIC have also motivated similar conclusions [21–24].

To facilitate comparison of these two collision systems, a scaled ratio between the XeXe and PbPb charged-particle spectra is defined as

$$R_{\mathrm{Pb}}^{\mathrm{Xe}}(p_T) = \frac{\mathrm{d}N^{\mathrm{XeXe}}/\mathrm{d}p_T}{\mathrm{d}N^{\mathrm{PbPb}}/\mathrm{d}p_T} \frac{T_{\mathrm{PbPb}}}{T_{\mathrm{XeXe}}}. \tag{1.3}$$

Here the AA notation is replaced with the names of the appropriate ion species. Unlike R_{AA}, this ratio does not depend on pp reference data. Because the PbPb data were gathered at $\sqrt{s_{\mathrm{NN}}} = 5.02\,\mathrm{TeV}$, the two collision systems compared in this paper have different center-of-mass energies. A deviation of $R_{\mathrm{Pb}}^{\mathrm{Xe}}$ from expected values, after taking this energy difference into account, would indicate a different spectral modification between XeXe and PbPb collisions.

In this paper, p_T spectra are reported for charged particles with pseudorapidity $|\eta| < 1$ in XeXe collisions at $\sqrt{s_{\mathrm{NN}}} = 5.44\,\mathrm{TeV}$. A pp reference spectrum at a center-of-mass energy ($\sqrt{s}$) of 5.44 TeV is constructed by extrapolating from an existing measurement at $\sqrt{s} = 5.02\,\mathrm{TeV}$ [17]. This reference is used to estimate the nuclear modification factor R_{AA}^*,

where the asterisk denotes the use of an extrapolated reference. The results for R^*_{AA} are compared to theoretical calculations, and potential implications are discussed.

2 The CMS detector

The central feature of the CMS apparatus is a superconducting solenoid of 6 m internal diameter, providing a magnetic field of 3.8 T. Within the solenoid volume are a silicon pixel and strip tracker, a lead tungstate crystal electromagnetic calorimeter, and a brass and scintillator hadron calorimeter, each composed of a barrel and two endcap sections. Forward calorimeters extend the η coverage provided by the barrel and endcap detectors. Muons are detected in gas-ionization chambers embedded in the steel flux-return yoke outside the solenoid.

The silicon tracker measures charged particles within the range $|\eta| < 2.5$. It consists of 1856 silicon pixel and 15 148 silicon strip detector modules. For nonisolated particles of $1 < p_{\mathrm{T}} < 10 \, \mathrm{GeV}$ and $|\eta| < 1.4$, the track resolutions are typically 25–90 (45–150) μm in the transverse (longitudinal) impact parameter [25].

The hadron forward (HF) calorimeter uses steel as an absorber and quartz fibers as the sensitive material. The two halves of the HF are located 11.2 m from the interaction region, one on each end, and together they provide coverage in the range $3.0 < |\eta| < 5.2$.

Events of interest are selected using a two-tiered trigger system [26]. During XeXe operation the first level trigger (L1), composed of custom hardware processors, uses information from the calorimeters to select events at a rate of around 4 kHz within a time interval of less than 4 μs. The second level, known as the high-level trigger (HLT), consists of a farm of processors running a version of the full event reconstruction software optimized for fast processing, and reduces the event rate to around 2 kHz before data storage.

A more detailed description of the CMS detector, together with a definition of the coordinate system used and the relevant kinematic variables, can be found in ref. [27].

3 Event samples and selections

This measurement uses XeXe data collected at $\sqrt{s_{\mathrm{NN}}} = 5.44 \, \mathrm{TeV}$ in 2017. During the six-hour data-taking period approximately 19 million minimum-bias (MB) events were gathered, corresponding to an integrated luminosity of 3.42 μb^{-1}. Events containing multiple XeXe collisions have a negligible effect on the measurement, as the average number of interactions per bunch crossing was less than 0.018. Events selected by the L1 trigger system were required to have a signal above the noise threshold in at least one of the two HF calorimeters. The HLT chose events having an energy deposit above approximately 1 GeV in the HF, as well as having at least one group of three pixel hits that is compatible with the trajectory of a charged particle originating from the luminous region. Every event passing these MB trigger conditions was recorded.

Samples of simulated XeXe Monte Carlo (MC) events are used to evaluate the detector performance and reconstruction efficiencies. Both MB EPOS [28] tune LHC [29] and HYDJET tuned with $\sqrt{s_{\mathrm{NN}}} = 5.02 \, \mathrm{TeV}$ PbPb MB events [30] are employed. An additional

Centrality	$\langle N_{\text{part}} \rangle$		$\langle N_{\text{coll}} \rangle$		T_{AA} [mb^{-1}]	
	XeXe	PbPb	XeXe	PbPb	XeXe	PbPb
0–5%	236.1 ± 1.3	$384.3^{+1.8}_{-2.0}$	930 ± 51	1820^{+130}_{-140}	13.60 ± 0.74	$26.0^{+0.5}_{-0.8}$
5–10%	206.3 ± 1.7	$333.3^{+3.0}_{-3.2}$	732 ± 44	1430^{+100}_{-110}	10.70 ± 0.65	$20.5^{+0.4}_{-0.6}$
10–30%	141.2 ± 1.8	$226.7^{+5.2}_{-5.3}$	407 ± 30	805^{+55}_{-58}	5.94 ± 0.44	$11.5^{+0.3}_{-0.4}$
30–50%	68.5 ± 2.2	$109.2^{+4.3}_{-4.2}$	135 ± 15	267^{+20}_{-20}	1.97 ± 0.22	$3.82^{+0.21}_{-0.21}$
50–70%	27.2 ± 1.6	$42.2^{+3.0}_{-2.9}$	35.3 ± 4.8	$65.4^{+7.0}_{-6.6}$	0.517 ± 0.071	$0.934^{+0.096}_{-0.089}$
70–80%	10.55 ± 0.78	—	9.8 ± 1.4	—	0.143 ± 0.020	—
70–90%	—	$11.1^{+1.3}_{-1.2}$	—	$10.7^{+1.7}_{-1.5}$	—	$0.152^{+0.024}_{-0.021}$
0–10%	221.2 ± 1.5	$358.8^{+2.4}_{-2.6}$	831 ± 47	1630^{+120}_{-120}	12.10 ± 0.69	$23.2^{+0.4}_{-0.7}$

Table 1. The values of $\langle N_{\text{part}} \rangle$, $\langle N_{\text{coll}} \rangle$, T_{AA}, and their uncertainties, for $\sqrt{s_{\text{NN}}} = 5.44$ TeV XeXe collisions and 5.02 TeV PbPb collisions in the centrality ranges used here.

set of HYDJET-embedded PYTHIA 8.230 [31] events (MB HYDJET events containing an additional hard scattering generated by PYTHIA tune CUETP8M1 [32]) is used to examine the reconstruction performance and p_{T} resolution for high-p_{T} charged particles.

A heavy ion collision centrality quantifies the amount of overlap between the two colliding ions. For both data and MC events, the centrality is estimated from the sum of the transverse energy deposited in both HF detectors. In this work, centrality selections are expressed as percentage ranges of the total hadronic inelastic cross section. Lower percentiles indicate a larger degree of overlap between the two nuclei. Thus, the 0–5% centrality range selects the most head-on XeXe collisions in the sample.

An event centrality is closely related to the number of participating nucleons, N_{part}, and the number of binary nucleon-nucleon collisions, N_{coll}, in the event. The $\langle N_{\text{part}} \rangle$, $\langle N_{\text{coll}} \rangle$, and corresponding T_{AA} for a given centrality range are calculated with a Glauber model of the nucleons contained in each ion [8]. For the purposes of this model, the nucleon-nucleon inelastic cross section $\sigma_{\text{NN}}^{\text{inel}}$ is taken as 68.4 ± 0.5 mb [33]. The nuclear radius and skin depth are set as 5.36 ± 0.1 fm and 0.59 ± 0.07 fm, respectively [19]. Additionally, the nuclear deformation parameter of the xenon nucleus is taken to be $\beta_2 = 0.18 \pm 0.02$ [34]. Simulated EPOS events are used to account for bin-to-bin smearing in centrality caused by fluctuations and the energy resolution of the HF calorimeters [8]. The resulting values and uncertainties are given in table 1 for XeXe collisions at $\sqrt{s_{\text{NN}}} = 5.44$ TeV. For the purpose of calculating $R_{\text{Pb}}^{\text{Xe}}$, the same quantities in PbPb collisions at 5.02 TeV are also given. The procedure for calculating the PbPb values is described in ref. [17]. The uncertainties in the PbPb values include a component related to the uncertainty in the PbPb event selection efficiency. However, the effect of the XeXe event selection efficiency uncertainty is much larger than in PbPb collisions. Therefore, this component is not propagated to the uncertainty in the XeXe values and is accounted for with a separate systematic uncertainty. In this paper, the definition of R_{AA} containing T_{AA}, given in eq. (1.2), is used.

In the offline analysis, events are required to have a reconstructed primary vertex that is formed from at least two tracks and is within 15 cm of the detector center. This rejects

background processes such as beam-gas collisions. The events must also have at least three detector elements containing energy deposits of at least 3 GeV in each of the two HF subdetectors. Finally, at least 25% of the tracks in an event must pass a track-quality selection [25]. These conditions, along with the MB trigger requirements, are estimated to select $(95 \pm 3)\%$ of the total inelastic cross section. This efficiency also includes potential contributions from ultraperipheral electromagnetic interactions contaminating the selected sample and was calculated using samples of EPOS, HYDJET, and STARLIGHT v2.2 [35]. In the 0–80% centrality range used for this analysis, the event selection is fully efficient and any remaining electromagnetic contamination is negligible.

4   Track reconstruction and corrections

The spectra measured here are for primary charged particles, defined as having an average proper lifetime greater than 1 cm. Daughters originating from secondary decays are not considered primary unless the mother particle has an average proper lifetime under 1 cm. The rate at which these nonprimary tracks contaminate the sample is estimated to be less than 0.3%. Particles coming from interactions with detector components are not included in the primary-particle definition.

Tracks and primary vertices are reconstructed using the procedures described in ref. [25]. Small modifications to these algorithms are made to facilitate the reconstruction of XeXe events having large track multiplicities. Tracks are required to be in the range $|\eta| < 1$. Poor-quality tracks are removed from the sample by applying strict track selections identical to the ones described for PbPb collisions in ref. [17]. Notably, these selections require each track with $p_T > 20$ GeV to be associated with a calorimeter energy deposit [36] of at least half the track's momentum. They also reject tracks having a significance of the distance of closest approach (DCA) to the primary vertex in the x-y plane that is greater than 3 standard deviations.

The tracking performance is evaluated using simulated HYDJET-embedded PYTHIA events and is found to be similar to the performance in PbPb collisions having similar detector occupancy. The track p_T resolution is <1.5% for the full p_T range of this study. The tracking efficiency, defined as the fraction of primary charged particles successfully reconstructed after track quality selections, is shown in figure 1. The shaded bands around each line show statistical uncertainties. The efficiency has a fairly constant value around 70% (76%) in the range $3 < p_T < 100$ GeV for central (peripheral) events. Because of the stringent track selection criteria, the efficiency decreases to a value of 13% at $p_T = 0.5$ GeV in the 0–5% centrality range, and to 30% in the 70–80% centrality range. The rate at which erroneous tracks not associated with a charged particle are generated, or the misreconstruction rate, is less than 1% for most of the p_T range studied. However, it does increase quickly for tracks having $p_T < 0.7$ GeV in the 0–5% centrality range, reaching a maximum value of 34% at $p_T = 0.5$ GeV. The effects of tracking inefficiency, misreconstruction, and nonprimary contamination are all corrected for by applying a weight to each track. This correction is parameterized as a function of the track p_T and event centrality.
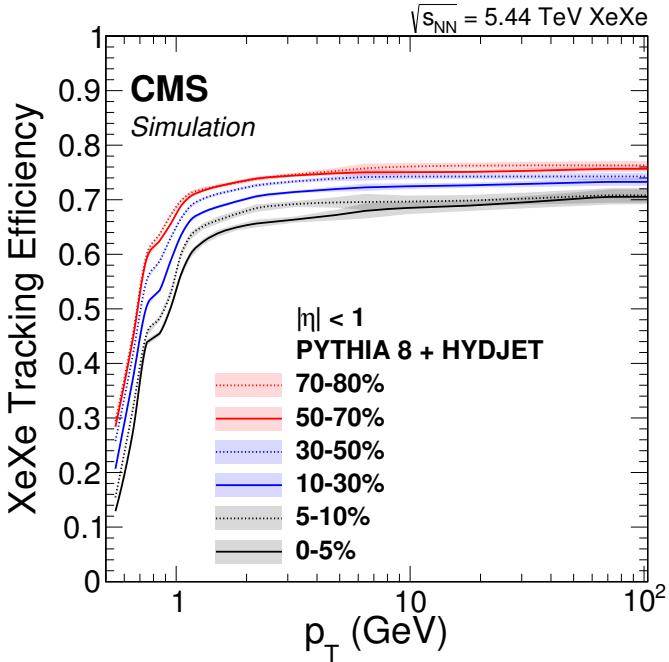
Figure 1. The XeXe tracking efficiency for six centrality selections. The tracking efficiency at low-p_T values decreases because of the strict track quality requirements used. Above $p_\mathrm{T} = 3\,\mathrm{GeV}$ the efficiency for central events is rather flat around 70%. The shaded bands show the statistical uncertainties.

The tracking efficiency for a charged particle at a given p_T depends on its species. Additionally, some charged particles, notably the strange baryons, are more likely to decay into secondary particles which then contaminate the sample. These effects lead to a model dependence of the total tracking correction, because different MC event generators predict dissimilar relative fractions of each type of charged particle. Notably, PYTHIA tends to underpredict strange hadron production in pp collisions [14], while EPOS is found to overestimate the production of many strange hadrons in central PbPb collisions [37]. Thus, the fraction of strange baryons in data is expected to be bounded by that of EPOS and of the embedded particles in a HYDJET-embedded PYTHIA sample. Following the procedure detailed in ref. [17], a working point is chosen that lies halfway between the tracking corrections produced by these two generators. The deviation between the estimated tracking corrections from the two generators reaches a maximum of 8% around $p_\mathrm{T} = 4\,\mathrm{GeV}$ but is less than 3% for $p_\mathrm{T} > 10\,\mathrm{GeV}$.

5 Reference spectrum

A reference spectrum from pp collisions at an appropriate center-of-mass energy is required to construct R_AA. Although no measurements exist at $\sqrt{s} = 5.44\,\mathrm{TeV}$, the CMS Collaboration has measured p_T spectra for collisions at $\sqrt{s} = 5.02\,\mathrm{TeV}$ [17] and 7 TeV [38]. An MC-based extrapolation procedure is applied to the 5.02 TeV spectrum because of its close proximity in energy to 5.44 TeV. The pp reference cross section used for the R_AA^*

calculation is

$$\left(\frac{\mathrm{d}\sigma_{5.44}^{\mathrm{pp}}}{\mathrm{d}p_{\mathrm{T}}}\right)_{\mathrm{Extrap.}} = \left(\frac{\mathrm{d}\sigma_{5.44}^{\mathrm{pp}}}{\mathrm{d}p_{\mathrm{T}}} \middle/ \frac{\mathrm{d}\sigma_{5.02}^{\mathrm{pp}}}{\mathrm{d}p_{\mathrm{T}}}\right)_{\mathrm{MC}} \left(\frac{\mathrm{d}\sigma_{5.02}^{\mathrm{pp}}}{\mathrm{d}p_{\mathrm{T}}}\right)_{\mathrm{Data}}. \qquad (5.1)$$

For most of the p_{T} range studied here, the charged-particle spectra for pp collisions produced by PYTHIA 8.223 tune CUETP8M1 were found to match data at $\sqrt{s} = 5.02$ and 7 TeV within the experimental uncertainties. Differences between the data and simulation for $p_{\mathrm{T}} < 1\,\mathrm{GeV}$ and around $p_{\mathrm{T}} = 10\,\mathrm{GeV}$ are similar at both center-of-mass energies and are expected to largely cancel in a ratio. Therefore, this generator is used for the reference reported here. The extrapolation factor is extracted by fitting a polynomial of the form $a_0 + a_1 x + a_2 x^2 + a_3 x^3 + a_4 x^4$, with $x = \ln(p_{\mathrm{T}}/1\,\mathrm{GeV})$, to the ratio of spectra at the two different center-of-mass energies. The fit parameters are $a_0 = 1.04$, $a_1 = 2.56 \times 10^{-2}$, $a_2 = 1.27 \times 10^{-2}$, $a_3 = -4.72 \times 10^{-3}$, and $a_4 = 4.80 \times 10^{-4}$. This functional form is chosen to give a good empirical description of the simulated data, as seen in figure 2, and is not guaranteed to be valid outside the range $0.5 < p_{\mathrm{T}} < 100\,\mathrm{GeV}$. The extrapolation factor spans the range from 1.03 at $p_{\mathrm{T}} = 0.5\,\mathrm{GeV}$ to 1.18 at $p_{\mathrm{T}} = 100\,\mathrm{GeV}$. For most of this p_{T} range, the fit's statistical uncertainty is smaller than the thickness of the red line in figure 2. The extrapolation procedure is checked at low-p_{T} using EPOS tune LHC, which is found to be within 1% of PYTHIA until around $p_{\mathrm{T}} = 10\,\mathrm{GeV}$. At higher p_{T}, a fit to HERWIG++[39] tune EE5C [32] deviates from the PYTHIA result by no more than 2%. Other functional forms including sigmoid functions and ratios of Tsallis distributions [40] are found to agree with the nominal fit to within 1%.

Alternative methods of calculating a reference spectrum were attempted. A similar extrapolation starting from data at $\sqrt{s} = 7\,\mathrm{TeV}$ is found to yield a reference spectrum within 5% of the one constructed using 5.02 TeV data. This difference is well within the experimental uncertainties of the 5.02 and 7 TeV data. The spectra produced by "relative placement" and x_T interpolation procedures [41] are tightly constrained by the existing 5.02 TeV measurement and are within 2% of the extrapolated reference cross section used here.

6 Systematic uncertainties

A breakdown of the systematic uncertainties related to measurements of the XeXe charged-particle p_{T} spectra, R_{AA}^* and $R_{\mathrm{Pb}}^{\mathrm{Xe}}$ is given in table 2. Systematic uncertainties that are fully correlated between points in a given centrality range are grouped together as normalization uncertainties and are not combined with other uncertainties. The ranges reported cover the span of each uncertainty across the p_{T} and centrality range of the measurement. A detailed discussion of each component of the systematic uncertainty is given below. References to the uncertainties in PbPb and pp collisions concern the measurements described in ref. [17].

- Fraction of misreconstructed tracks. The misreconstruction rate is evaluated in simulated events. To account for potential deviations from this value in data, the distribution of the significance of the tracks' DCA to the primary vertex in the x-y
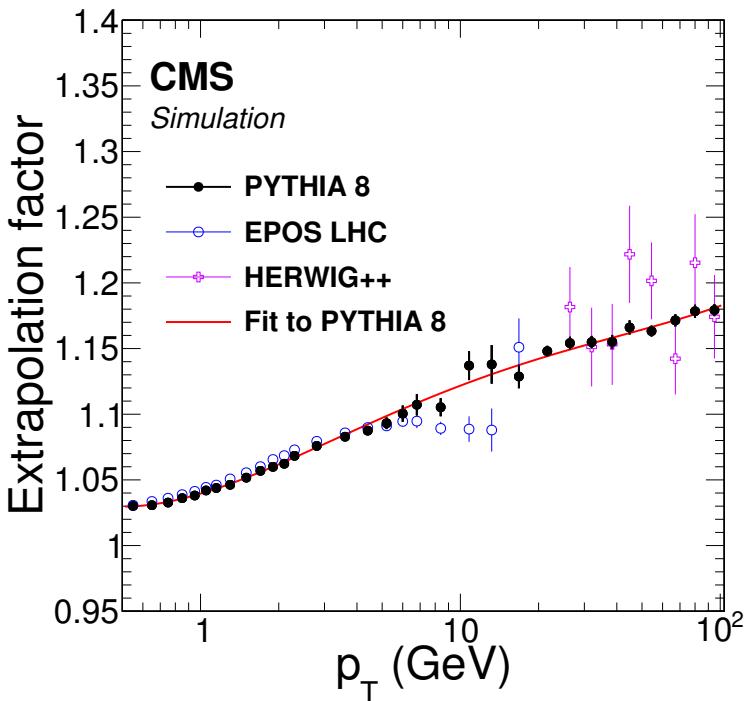
Figure 2. The ratio of charged-particle spectra in pp collisions at $\sqrt{s} = 5.44$ and $5.02\,\mathrm{TeV}$ for three different MC generators. A fit to the PYTHIA ratio is shown by the red line.

Sources	Uncertainty [%]		
	XeXe Spectra	R_{AA}^{*}	$R_{\mathrm{Pb}}^{\mathrm{Xe}}$
Fraction of misreconstructed tracks	0.1–16	0.1–16	0.1–5
Particle species composition	0.5–8	0.5–8	1–8
Track selection	3–6	3–6	5–7
MC/data tracking efficiency difference	5	2.0–6.4	—
Tracking corrections	0.5–2	0.5–2	1–5
p_{T} resolution	0.5	0.5	—
Extrapolated pp reference	—	4–9	—
Trigger combination	—	—	1
Combined uncertainty	7–18	6–18	6–11
XeXe event selection efficiency	0.3–26	0.3–26	0.3–26
Glauber model uncertainty (T_{AA})	—	5–14	6–21
pp reference luminosity	—	2.3	—
Combined normalization uncertainty	0.3–26	6–30	6–33

Table 2. The systematic uncertainties related to the measurements reported here. The values quoted cover the centrality and p_{T} dependence of each uncertainty. They are separated into normalization uncertainties and all other systematic uncertainties.

plane is examined. The relative contribution of misreconstructed tracks to this distribution is scaled in simulated events to match data in a sideband region having a DCA significance between 25 and 30 standard deviations. Tracks in this region are almost entirely misreconstructed tracks, and therefore give an estimate of the difference in the misreconstruction effect between data and simulation. After this scaling procedure, the relative change of the misreconstruction rate in the signal region (less than 3 standard deviations) is taken as the systematic uncertainty. This is $< 2\%$ for most of the data in this analysis. For tracks having $p_{\mathrm{T}} < 0.7\,\mathrm{GeV}$ in central events, however, it quickly grows to a value of 16%.

- Particle species composition. The correction applied to account for the model-dependence of the tracking correction assumes the particle composition of data lies somewhere between PYTHIA and EPOS. To cover the range spanned by both of these models, the difference between the two tracking corrections produced by these models is taken as an approximate estimate of the uncertainty. This uncertainty strongly peaks around $4\,\mathrm{GeV}$, where the difference in particle composition is the largest for the two generators. At $p_{\mathrm{T}} > 10\,\mathrm{GeV}$, where the two generators converge, a systematic uncertainty of 3% is assigned. No cancellation of this uncertainty is assumed for R_{AA}^*. The uncertainties are correlated in PbPb and XeXe collisions and are partially canceled for $R_{\mathrm{Pb}}^{\mathrm{Xe}}$.

- Track selection. Differences between data and MC track distributions cause the same track selections to remove slightly different numbers of particles. The sensitivity of the analysis to this effect is checked by varying the strictness of the track selection criteria. An uncertainty of 6% is assigned for this effect under $p_{\mathrm{T}} = 20\,\mathrm{GeV}$. For higher p_{T} values the uncertainty is only 3%. This uncertainty is conservatively assumed to not cancel in the ratios measured, and a similar uncertainty for PbPb collisions is included for $R_{\mathrm{Pb}}^{\mathrm{Xe}}$.

- MC/data tracking efficiency difference. An uncertainty of 5% is assigned for additional differences in the tracking efficiency not related to the particle fractions modeled in MC events. These differences could be related to small variations in the detector conditions or slight inaccuracies in the simulation of the detector. This uncertainty is estimated using measurements of the relative tracking efficiency in decays of D^* mesons in pp collisions, along with studies of the relative tracking efficiency's occupancy-dependence in PbPb collisions. For R_{AA}^* this systematic uncertainty is conservatively assumed to cancel as much as it did for previous analyses in PbPb collisions [17], giving an uncertainty of 2.0 (6.4)% for peripheral (central) events. This uncertainty largely cancels in $R_{\mathrm{Pb}}^{\mathrm{Xe}}$, where the occupancies of the two systems in the ratio are more similar than in R_{AA}^*.

- Tracking corrections. The statistical uncertainty in the tracking corrections, caused by the finite size of the XeXe MC samples used, is accounted for as a systematic uncertainty in the final results. This uncertainty is between 0.5% and 2.0%. A

similar uncertainty covering MC sample size and tracking correction procedures in PbPb collisions is added in quadrature to this uncertainty for $R_{\text{Pb}}^{\text{Xe}}$.

- Transverse momentum resolution. The distortion of the p_{T} spectra caused by detector resolution was evaluated with simulated events. A systematic uncertainty of 0.5% accounts for potential changes in the yield of any given p_{T} bin. Because of the similarity in shape of the XeXe and PbPb spectra, this uncertainty cancels for $R_{\text{Pb}}^{\text{Xe}}$.

- Extrapolated pp reference. The total uncertainty in the extrapolated pp reference cross section at 5.44 TeV is dominated by the 7–10% uncertainty in the original measurement at 5.02 TeV. This uncertainty includes a fully correlated 2.3% uncertainty in the total integrated luminosity [42] that is included as a normalization uncertainty in figures displaying R_{AA}^{*}. For the purposes of calculating R_{AA}^{*}, the MC/data track efficiency difference and p_{T} resolution components of this uncertainty, which partially cancel with XeXe uncertainties, are removed from the pp reference data uncertainty and included elsewhere to avoid double counting. An additional 1% uncertainty is included to account for variations in the functional form used to fit the simulation-based extrapolation factor.

- Trigger combination. The XeXe data used in this analysis were collected with only one MB trigger, so there is no uncertainty related to using multiple triggers to select XeXe events. However, the trigger scheme used to measure the PbPb spectra used in the $R_{\text{Pb}}^{\text{Xe}}$ calculation has a 1% uncertainty associated with it.

- XeXe event selection efficiency. The 3% uncertainty on the total XeXe event selection efficiency is propagated to the results by repeating the analysis after appropriately varying the centrality calibration. These variations each cause a shift in the centrality values of the entire data sample, with peripheral centralities being altered significantly more than central ones. Therefore, this uncertainty is small for central events but grows with the collision centrality. In the 70–80% centrality range it reaches values of 26%. The uncertainty is fully correlated across all p_{T} values in a given centrality selection.

- Glauber model uncertainty. The uncertainty in T_{AA} for XeXe collisions ranges from 5% to 14%. This uncertainty is calculated by propagating uncertainties in the Glauber model's input parameters, which are detailed in section 3. The uncertainty in the XeXe collision event selection efficiency is not included because it is accounted for with a separate systematic uncertainty. The uncertainty in the quantity $T_{\text{PbPb}}/T_{\text{XeXe}}$, used in $R_{\text{Pb}}^{\text{Xe}}$, is determined by adding in quadrature the relative uncertainties in T_{AA} for each collision system.

7   Results

Charged-particle p_{T} spectra in XeXe collisions at $\sqrt{s_{\text{NN}}} = 5.44$ TeV are shown in figure 3 for six centrality ranges. The data are reported as per-event invariant differential yields.
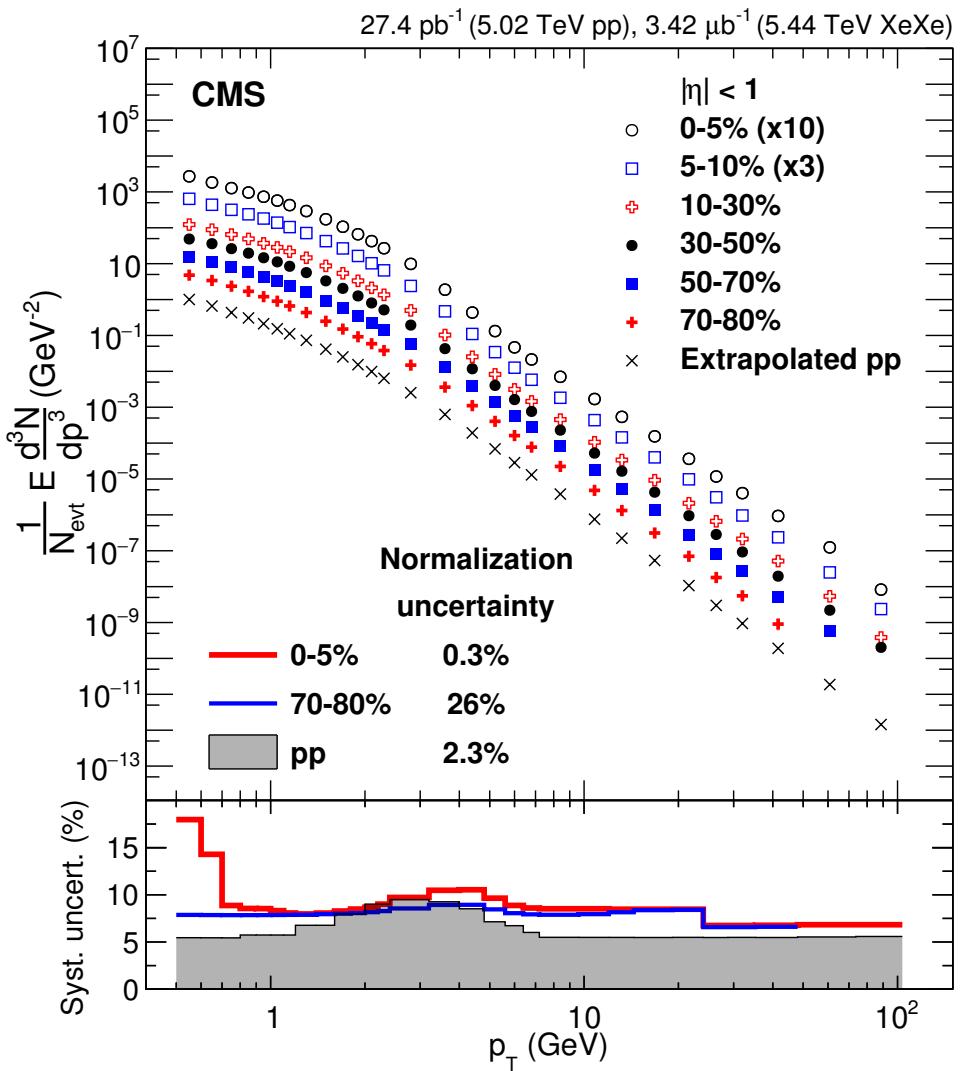
Figure 3. (Upper panel) The charged-particle p_{T} spectra in six classes of XeXe centrality and the pp reference spectrum after being extrapolated to $\sqrt{s} = 5.44\,\mathrm{TeV}$. The statistical uncertainties are smaller than the markers for many of the points. To facilitate direct comparison, the pp points are converted to per-event yields using a constant factor of 70 mb. (Lower panel) The systematic uncertainties for central and peripheral XeXe collisions, as well as for the pp reference data.

To improve visual clarity, the spectra for the 0–5% and 5–10% centrality ranges have been scaled by ten and three, respectively. The extrapolated pp reference data for the same center-of-mass energy is also reported. The reference used for R_{AA}^{*} is a differential cross section, but has been converted to a per-event yield using a constant factor of 70 mb to allow for direct comparison in figure 3. The data points represent the average charged-particle yield in each p_{T} bin, not the charged-particle yield at the bin center where the point is placed. The statistical uncertainties of the measurement are smaller than the markers for most of the data points. The pp reference spectrum has a shape similar to that of a Tsallis distribution, including a power law behavior at large p_{T} values. This is consistent

with earlier observations that this functional form is able to describe charged-particle p_T spectra at LHC energies [40]. The lower panel of figure 3 shows the systematic uncertainties for the most central and peripheral XeXe collisions, and for the extrapolated pp reference data. A few values of the systematic uncertainties in the normalization of the spectra are also listed.

The resulting R^*_{AA} values for primary charged particles in XeXe collisions are shown in figure 4. The pink boxes represent all systematic uncertainties other than the uncertainty in the overall normalization, which is shown by the dark red box around unity. The error bars give the statistical uncertainty of the measurement. For comparison, the R_{AA} in PbPb collisions at $\sqrt{s_{NN}} = 5.02\,\text{TeV}$ [17] is shown by the hollow blue points. The blue boxes represent the systematic uncertainties of the PbPb data. The most central events show a strong modification that is most pronounced in the range $5 < p_T < 30\,\text{GeV}$. A similar oscillatory shape is observed in both XeXe and PbPb collisions, indicating that hot medium effects seen in PbPb collisions are also present in XeXe collisions. At low p_T, these effects include contributions from the nuclear parton distribution function [43], radial flow [44], and the Cronin effect [45]. At higher p_T, parton energy loss also becomes a significant effect. Generally, R_{AA} and R^*_{AA} agree with each other in the range $p_T < 4\,\text{GeV}$. However, the data may indicate a slight difference in suppression levels at higher p_T. As the centrality range examined becomes more peripheral, the oscillating shape of R^*_{AA} becomes less pronounced. In the most peripheral collisions examined, the XeXe data are relatively flat, indicating that the spectral shape for peripheral centrality ranges is similar to that of pp collisions. Although there is a large normalization uncertainty, the R^*_{AA} is significantly below unity in this centrality range. Such a suppression in peripheral events is not expected to be caused by strong energy loss effects, but might be related to correlations between the charged-particle yields in the mid-rapidity region with event activity in the range $3 < |\eta| < 5.2$ that is used to determine the event centrality [46]. Recent measurements of R_{AA} in peripheral PbPb collisions by the ALICE Collaboration show a similar effect that has been interpreted as a bias caused by event selection and collision geometry [47]. Studies in MB HYDJET indicate this bias could be as large as 50% at high p_T in the 70–80% centrality range, but is expected to be less than 10% for more central events. This peripheral suppression could also be caused by a bias in T_{AA} values if the spatial distribution of hard partons inside each nucleus is narrower than expected [48].

The difference in the suppression between R_{AA} for PbPb collisions and R^*_{AA} in XeXe collisions can be directly compared with the ratio R^{Xe}_{Pb}. Using the PbPb charged-particle spectra from ref. [17], this quantity is determined for five centrality ranges and shown in figure 5. The dark red box around unity shows the relative normalization uncertainty in the results. The MC-based pp extrapolation factor used in the construction of R^*_{AA} is represented by the blue line, and shows the expected deviation of R^{Xe}_{Pb} from unity resulting from the different center-of-mass energies of the two collision systems. In central events, the data for charged particles having $p_T < 4\,\text{GeV}$ are consistent with this expectation. However, there is a sudden rise in R^{Xe}_{Pb} in the range of $5 < p_T < 10\,\text{GeV}$, up to a value of 1.45. This excess does not appear to be caused by the center-of-mass energy dependence and is located in the p_T region where R^*_{AA} is the most suppressed. This suggests a difference
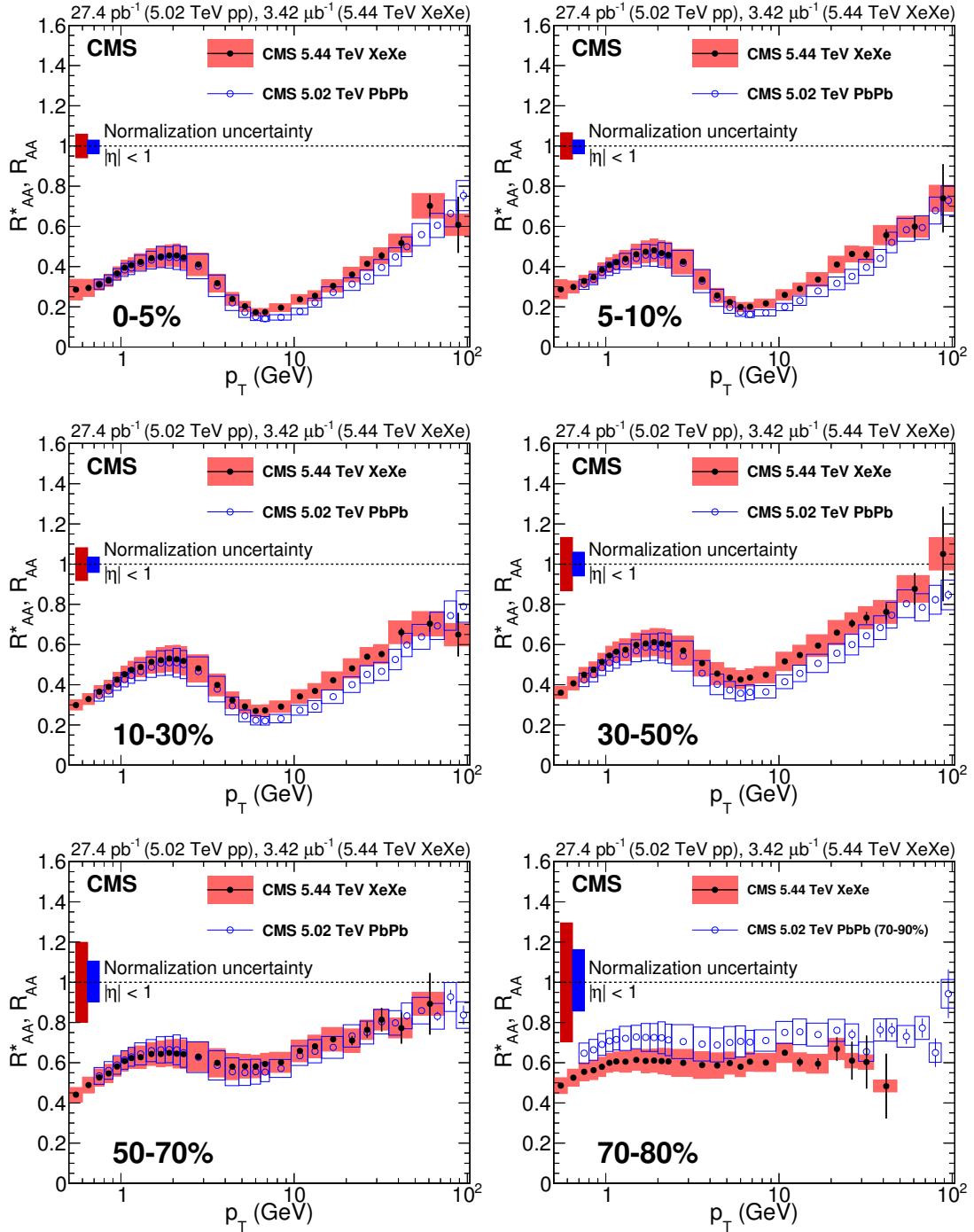
Figure 4. The charged-particle R^*_{AA} for XeXe collisions at $\sqrt{s_{NN}} = 5.44\,\text{TeV}$ in six centrality ranges. A previous measurement of R_{AA} in PbPb collisions at $5.02\,\text{TeV}$ is also shown [17]. The solid pink and open blue boxes represent the systematic uncertainties of the XeXe and PbPb data, respectively.
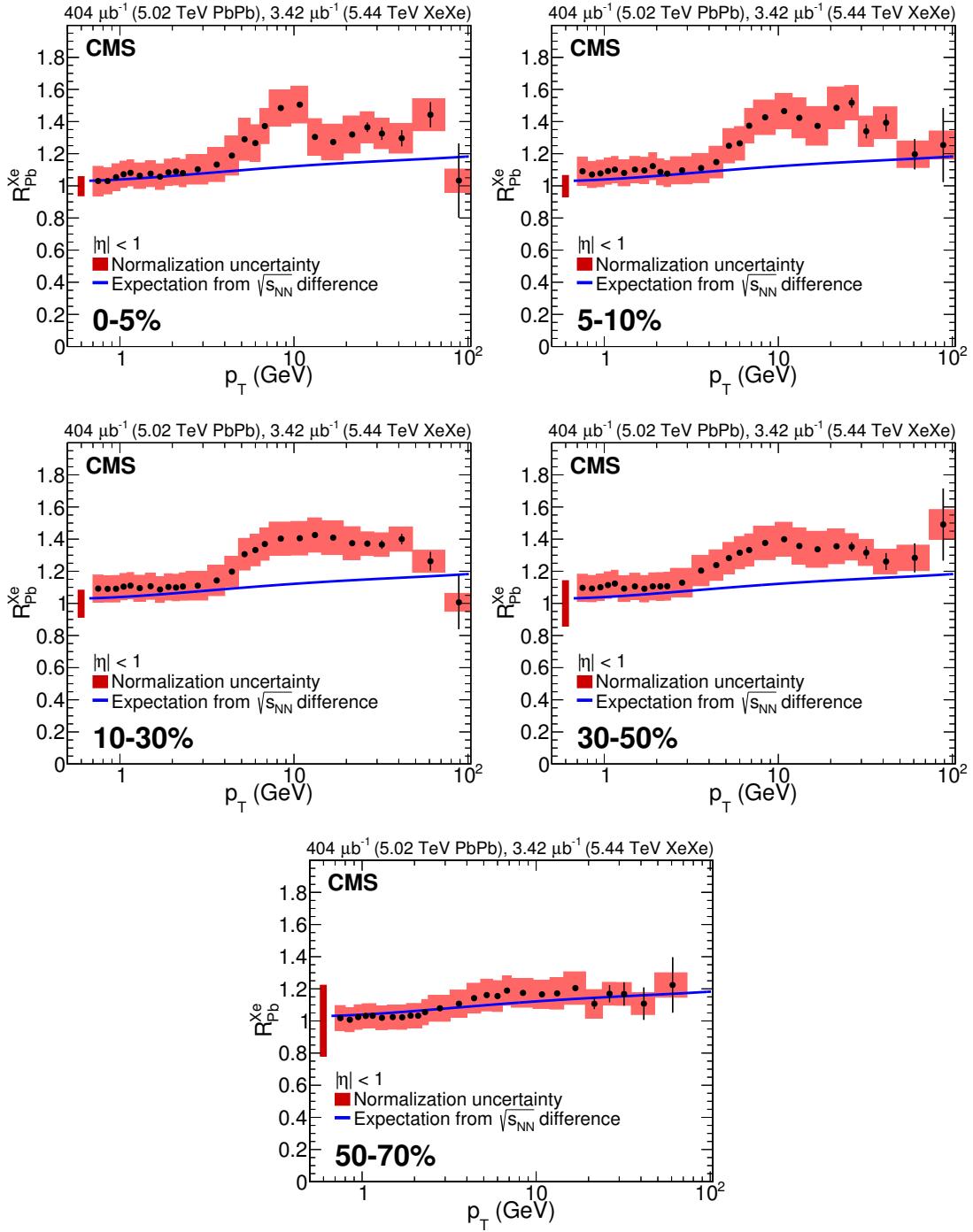
Figure 5. The measurement of $R^{\mathrm{Xe}}_{\mathrm{Pb}}$ in five centrality classes using the results of this analysis and data from ref. [17]. The blue line represents the expected deviation from unity caused by the different center-of-mass energies of the two collision systems. The solid pink boxes represent the systematic uncertainties.
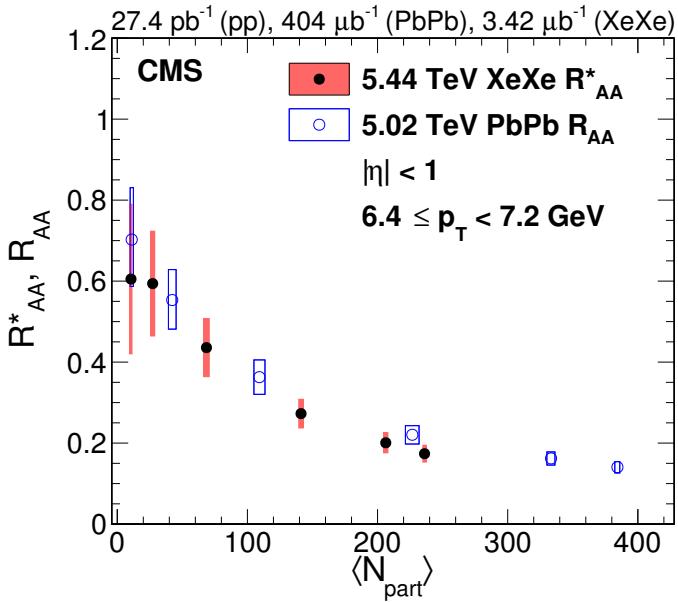
Figure 6. The charged-particle R^*_{AA} for XeXe collisions at $\sqrt{s_{NN}} = 5.44\,\text{TeV}$ and R_{AA} for PbPb collisions at $5.02\,\text{TeV}$, as a function of $\langle N_{\text{part}} \rangle$. The solid pink and open blue boxes represent the total systematic uncertainties in the XeXe and PbPb data, respectively.

in the strength of energy loss in the two collision systems, which could be caused by the difference in the system size. As the p_T increases towards $100\,\text{GeV}$, the data slowly converge towards the values expected from the difference in the center-of-mass energy. As the centrality range examined becomes more peripheral, the excess seen around 5 to $10\,\text{GeV}$ decreases in strength. In the most peripheral bins, R^{Xe}_{Pb} is consistent with the difference expected because of the center-of-mass energies throughout the entire p_T range.

Because xenon ions are smaller than lead ions, collisions at the same centrality will contain a different numbers of participating nucleons. To compare XeXe and PbPb collisions having a similar number of colliding nucleons, the values of R_{AA} and R^*_{AA} for $6.4 \leq p_T < 7.2\,\text{GeV}$ are shown as a function of $\langle N_{\text{part}} \rangle$ in figure 6. The chosen p_T range corresponds to the minima of R_{AA} and R^*_{AA}. The boxes surrounding the data points show the total systematic uncertainties in the measurements. The R_{AA} and R^*_{AA} values seem to follow a similar trend versus $\langle N_{\text{part}} \rangle$. In particular, the values of R_{AA} and R^*_{AA} around $\langle N_{\text{part}} \rangle = 220$ are compatible within the uncertainties.

Measurements of R^{Xe}_{Pb} that compare data having similar $\langle N_{\text{part}} \rangle$, rather than centrality, are shown in figure 7. The left panel compares 0–5% XeXe collisions with 10–30% PbPb collisions, which have $\langle N_{\text{part}} \rangle$ values of 236.1 ± 1.3 and $226.7^{+5.2}_{-5.3}$, respectively. In this case, the R^{Xe}_{Pb} values are slightly below the expectation from the different center-of-mass energies for $p_T < 20\,\text{GeV}$, but are compatible with the expectation at higher p_T. In the p_T range of 3–8 GeV, this ratio exhibits a slightly decreasing trend instead of the sharp rise seen when comparing similar centrality bins, reinforcing the conclusion that such a rise is due to a difference in the system size. The right plot compares 70–80% XeXe events with 70–90% PbPb events. In these centrality ranges, the $\langle N_{\text{part}} \rangle$ value is 10.55 ± 0.78 for XeXe collisions
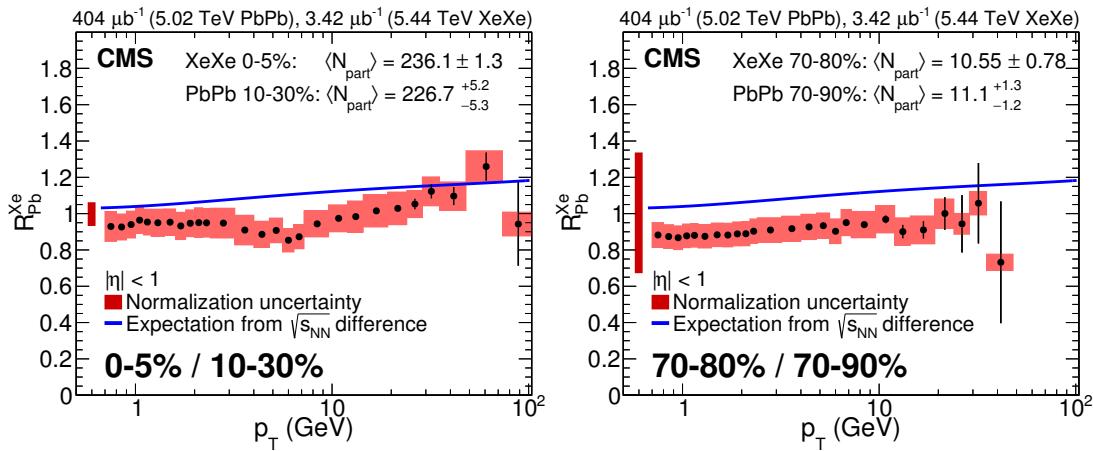
Figure 7. Measurements of $R_{\mathrm{Pb}}^{\mathrm{Xe}}$ comparing centrality ranges having similar values of $\langle N_{\mathrm{part}} \rangle$. The blue line represents the expected deviation from unity caused by the different center-of-mass energies of the two collision systems. The solid pink boxes represent the systematic uncertainties.

and $11.1_{-1.2}^{+1.3}$ for PbPb events. The measurement has a large normalization uncertainty, but the shape of the distribution is very similar to the trend given by the center-of-mass energy difference of the two systems.

The R_{AA}^{*} values in the 0–10% and 30–50% ranges are compared to various theoretical models in figure 8. A ratio of each model to the data is provided in the bottom panels of the figure. The green lines show the predictions of a linear Boltzmann transport (LBT) model of jet quenching, which uses the CLV$_{\mathrm{ISC}}$ hydrodynamics model for medium evolution [49, 50]. This model predicts a quadratic path-length dependence of energy loss in a static medium. It lies on the upper edge of the systematic uncertainty of the 0–10% measurement in the range $20 < p_{\mathrm{T}} < 60\,\mathrm{GeV}$, but otherwise agrees with the data well. The orange band is a model by Djordjevic that uses a dynamical energy loss formalism [51, 52]. For this model, the medium undergoes Bjorken expansion, and the path-length dependence of energy loss is expected to be between linear and quadratic. The prediction is compatible with the data in both centrality ranges except around $p_{\mathrm{T}} = 5\,\mathrm{GeV}$, where it is slightly below the data. The magenta region represents the prediction from CUJET3.1/CIBJET model, which incorporates two components [53, 54]. The first is a jet quenching model (CUJET3.1) that includes the suppression of quark and gluon degrees of freedom and the emergence of chromo-magnetic monopole degrees of freedom. The second component, the CIBJET framework, calculates the dependence of correlations between soft and hard azimuthal flow harmonics on an event-by-event basis. This model describes the 0–10% data well, but lies on the lower edge of the data's uncertainty in the 30–50% centrality range. The red line shows a prediction of Andrés et al. that uses a 'quenching weights' formalism to estimate the behavior of the medium transport coefficient, $\hat{q}$ [55]. The evolution of the medium in this model is done with EKRT event-by-event hydrodynamics. The prediction tends to agree with the top edge of the data's uncertainty range in the 0–10% centrality range. The light blue band shows a prediction from soft-collinear effective theory with Glauber gluons (SCET$_{\mathrm{G}}$) [56, 57]. The evolution of the background medium is modeled with the
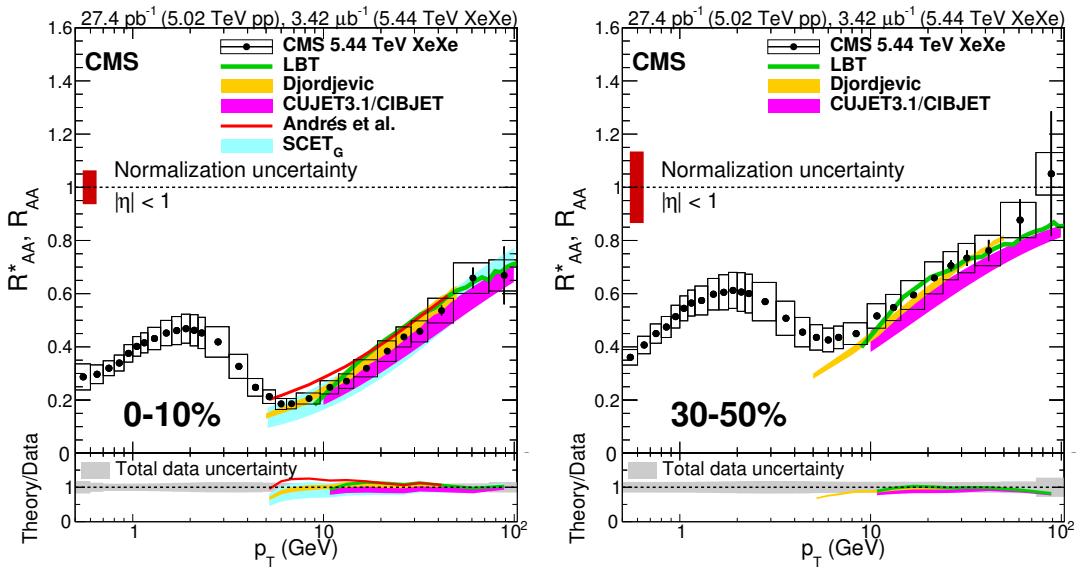
Figure 8. A comparison of the charged-particle R^*_{AA} for XeXe collisions at $\sqrt{s_{NN}} = 5.44\,\text{TeV}$ with theoretical predictions from refs. [49–57] for 0–10% (left) and 30–50% (right) centrality classes. The hollow black boxes represent the systematic uncertainties of the XeXe data. Ratios are shown in the bottom panels, where the gray band represents the total uncertainty in the measurement.

IEBE hydrodynamics package. In this model, R_{AA} is found to scale roughly as $N_{\text{part}}^{2/3}$. For central events, it slightly underestimates the R^*_{AA} around 5 GeV, but generally agrees with the data.

8 Summary

The transverse momentum, p_T, spectra of charged particles in the pseudorapidity range $|\eta| < 1$ are measured in several ranges of collision centrality for xenon-xenon (XeXe) collisions at a center-of-mass energy per nucleon pair of 5.44 TeV. A proton-proton (pp) reference spectrum for the same energy is extrapolated from an existing measurement at $\sqrt{s} = 5.02\,\text{TeV}$ using a scaling function calculated from simulated PYTHIA events. The nuclear modification factor with extrapolated reference, R^*_{AA}, is constructed from these spectra. In central events, R^*_{AA} has a value of 0.17 in the p_T range of 6–8 GeV, before increasing to a value of around 0.7 at 100 GeV. This suppression is less than what has been observed in a matching centrality range of lead-lead (PbPb) collisions at a center-of-mass energy per nucleon pair of 5.02 TeV, even when accounting for the difference in collision energy. In contrast, charged-particle production in XeXe collisions is found to be slightly more suppressed than in PbPb collisions that have a similar number of participating nucleons rather than a similar centrality. Taken together, these observations illustrate the importance that collision system size and geometry have on the strength of parton energy loss. Predictions from the Djordjevic, SCET$_G$ and CUJET3.1/CIBJET models are found to agree with the measured R^*_{AA}. The model of Andrés et al. lies on the upper edge of the systematic uncertainties of R^*_{AA} for central events. Finally, calculations using a

linear Boltzmann transport model also agree with the data, except for the kinematic range $15 < p_{\mathrm{T}} < 40\,\mathrm{GeV}$ in central events, where they follow the upper edge of the data's uncertainty. These measurements help elucidate the nature of parton energy loss in XeXe collisions and constrain the system size dependence of hot nuclear medium effects.

Acknowledgments

References

[1] G.-Y. Qin and X.-N. Wang, *Jet quenching in high-energy heavy-ion collisions*, *Int. J. Mod. Phys.* **E 24** (2015) 1530014 [arXiv:1511.00790] [INSPIRE].

[2] J.D. Bjorken, *Energy loss of energetic partons in quark-gluon plasma: possible extinction of high p_T jets in hadron-hadron collisions*, FERMILAB-PUB-82-059-T (1982).

[3] D. d'Enterria, *Jet quenching*, in *Relativistic heavy ion physics*, R. Stock ed., Landolt-Börnstein, Springer Germany (2010), arXiv:0902.2011.

[4] M. Gyulassy, I. Vitev and X.N. Wang, *High p_T azimuthal asymmetry in noncentral A+A at RHIC*, *Phys. Rev. Lett.* **86** (2001) 2537 [nucl-th/0012092] [INSPIRE].

[5] A.M. Poskanzer and S.A. Voloshin, *Methods for analyzing anisotropic flow in relativistic nuclear collisions*, *Phys. Rev.* **C 58** (1998) 1671 [nucl-ex/9805001] [INSPIRE].

[6] J.-Y. Ollitrault, *Anisotropy as a signature of transverse collective flow*, *Phys. Rev.* **D 46** (1992) 229 [INSPIRE].

[7] P.F. Kolb, J. Sollfrank and U.W. Heinz, *Anisotropic transverse flow and the quark hadron phase transition*, *Phys. Rev.* **C 62** (2000) 054909 [hep-ph/0006129] [INSPIRE].

[8] M.L. Miller, K. Reygers, S.J. Sanders and P. Steinberg, *Glauber modeling in high energy nuclear collisions*, *Ann. Rev. Nucl. Part. Sci.* **57** (2007) 205 [nucl-ex/0701025] [INSPIRE].

[9] BRAHMS collaboration, I. Arsene et al., *Quark gluon plasma and color glass condensate at RHIC? The perspective from the BRAHMS experiment*, *Nucl. Phys.* **A 757** (2005) 1 [nucl-ex/0410020] [INSPIRE].

[10] B.B. Back et al., *The PHOBOS perspective on discoveries at RHIC*, *Nucl. Phys.* **A 757** (2005) 28 [nucl-ex/0410022] [INSPIRE].

[11] STAR collaboration, J. Adams et al., *Experimental and theoretical challenges in the search for the quark gluon plasma: the STAR collaboration's critical assessment of the evidence from RHIC collisions*, *Nucl. Phys.* **A 757** (2005) 102 [nucl-ex/0501009] [INSPIRE].

[12] PHENIX collaboration, K. Adcox et al., *Formation of dense partonic matter in relativistic nucleus-nucleus collisions at RHIC: Experimental evaluation by the PHENIX collaboration*, *Nucl. Phys.* **A 757** (2005) 184 [nucl-ex/0410003] [INSPIRE].

[13] ALICE collaboration, *Centrality dependence of charged particle production at large transverse momentum in Pb-Pb Collisions at* $\sqrt{s_{NN}} = 2.76$ *TeV*, *Phys. Lett.* **B 720** (2013) 52 [arXiv:1208.2711] [INSPIRE].

[14] ALICE collaboration, *Transverse momentum spectra and nuclear modification factors of charged particles in pp, p-Pb and Pb-Pb collisions at the LHC*, arXiv:1802.09145 [INSPIRE].

[15] ATLAS collaboration, *Measurement of charged-particle spectra in Pb+Pb collisions at* $\sqrt{s_{NN}} = 2.76$ *TeV with the ATLAS detector at the LHC*, *JHEP* **09** (2015) 050 [arXiv:1504.04337] [INSPIRE].

[16] CMS collaboration, *Study of high-p_T charged particle suppression in PbPb compared to pp collisions at* $\sqrt{s_{NN}} = 2.76$ *TeV*, *Eur. Phys. J.* **C 72** (2012) 1945 [arXiv:1202.2554] [INSPIRE].

[17] CMS collaboration, *Charged-particle nuclear modification factors in PbPb and pPb collisions at* $\sqrt{s_{NN}} = 5.02$ *TeV*, *JHEP* **04** (2017) 039 [arXiv:1611.01664] [INSPIRE].

[18] ATLAS collaboration, *Transverse momentum, rapidity and centrality dependence of inclusive charged-particle production in* $\sqrt{s_{NN}} = 5.02$ *TeV p + Pb collisions measured by the ATLAS experiment*, *Phys. Lett.* **B 763** (2016) 313 [arXiv:1605.06436] [INSPIRE].

[19] C. Loizides, J. Nagle and P. Steinberg, *Improved version of the PHOBOS Glauber Monte Carlo*, *SoftwareX* **1-2** (2015) 13 [arXiv:1408.2549] [INSPIRE].

[20] ALICE collaboration, *Transverse momentum spectra and nuclear modification factors of charged particles in Xe-Xe collisions at* $\sqrt{s_{NN}} = 5.44$ *TeV*, arXiv:1805.04399 [INSPIRE].

[21] BRAHMS collaboration, I.C. Arsene et al., *Rapidity and centrality dependence of particle production for identified hadrons in Cu+Cu collisions at* $\sqrt{s_{NN}} = 200$ *GeV*, *Phys. Rev.* **C 94** (2016) 014907 [arXiv:1602.01183] [INSPIRE].

[22] PHOBOS collaboration, B. Alver et al., *System size and centrality dependence of charged hadron transverse momentum spectra in Au+Au and Cu+Cu collisions at* $\sqrt{s_{NN}} = 62.4$ *GeV and* 200 *GeV*, *Phys. Rev. Lett.* **96** (2006) 212301 [nucl-ex/0512016] [INSPIRE].

[23] PHENIX collaboration, A. Adare et al., *Onset of π^0 suppression studied in Cu+Cu collisions at* $\sqrt{s_{NN}} = 22.4$, 62.4 *and* 200 *GeV*, *Phys. Rev. Lett.* **101** (2008) 162301 [arXiv:0801.4555] [INSPIRE].

[24] STAR collaboration, B.I. Abelev et al., *Spectra of identified high-p_T $\pi^\pm$ and $p(\bar{p})$ in Cu+Cu collisions at* $\sqrt{s_{NN}} = 200$ *GeV*, *Phys. Rev.* **C 81** (2010) 054907 [arXiv:0911.3130] [INSPIRE].

[25] CMS collaboration, *Description and performance of track and primary-vertex reconstruction with the CMS tracker*, 2014 *JINST* **9** P10009 [arXiv:1405.6569] [INSPIRE].

[26] CMS collaboration, *The CMS trigger system*, 2017 *JINST* **12** P01020 [arXiv:1609.02366] [INSPIRE].

[27] CMS collaboration, *The CMS experiment at the CERN LHC*, 2008 *JINST* **3** S08004 [INSPIRE].

[28] K. Werner, F.-M. Liu and T. Pierog, *Parton ladder splitting and the rapidity dependence of transverse momentum spectra in deuteron-gold collisions at RHIC*, *Phys. Rev.* **C 74** (2006) 044902 [hep-ph/0506232] [INSPIRE].

[29] T. Pierog, I. Karpenko, J.M. Katzy, E. Yatsenko and K. Werner, *EPOS LHC: test of collective hadronization with data measured at the CERN Large Hadron Collider*, *Phys. Rev.* **C 92** (2015) 034906 [arXiv:1306.0121] [INSPIRE].

[30] I.P. Lokhtin and A.M. Snigirev, *A model of jet quenching in ultrarelativistic heavy ion collisions and high-p_T hadron spectra at RHIC*, *Eur. Phys. J.* **C 45** (2006) 211 [hep-ph/0506189] [INSPIRE].

[31] T. Sjöstrand, S. Mrenna and P.Z. Skands, *A brief introduction to PYTHIA 8.1*, *Comput. Phys. Commun.* **178** (2008) 852 [arXiv:0710.3820] [INSPIRE].

[32] CMS collaboration, *Event generator tunes obtained from underlying event and multiparton scattering measurements*, *Eur. Phys. J.* **C 76** (2016) 155 [arXiv:1512.00815] [INSPIRE].

[33] C. Loizides, J. Kamin and D. d'Enterria, *Improved Monte Carlo Glauber predictions at present and future nuclear colliders*, *Phys. Rev.* **C 97** (2018) 054910 [arXiv:1710.07098] [INSPIRE].

[34] ALICE collaboration, *Centrality and pseudorapidity dependence of the charged-particle multiplicity density in Xe-Xe collisions at $\sqrt{s_{NN}} = 5.44$ TeV*, arXiv:1805.04432 [INSPIRE].

[35] S.R. Klein et al., *STARlight: A Monte Carlo simulation program for ultra-peripheral collisions of relativistic ions*, *Comput. Phys. Commun.* **212** (2017) 258 [arXiv:1607.03838] [INSPIRE].

[36] CMS collaboration, *Particle-flow reconstruction and global event description with the CMS detector*, 2017 *JINST* **12** P10003 [arXiv:1706.04965] [INSPIRE].

[37] ALICE collaboration, *Multi-strange baryon production at mid-rapidity in Pb-Pb collisions at $\sqrt{s_{NN}} = 2.76$ TeV*, *Phys. Lett.* **B 728** (2014) 216 [*Erratum ibid.* **B 734** (2014) 409] [arXiv:1307.5543] [INSPIRE].

[38] CMS collaboration, *Charged particle transverse momentum spectra in pp collisions at $\sqrt{s} = 0.9$ and 7 TeV*, *JHEP* **08** (2011) 086 [arXiv:1104.3547] [INSPIRE].

[39] M. Bahr et al., *HERWIG++ physics and manual*, *Eur. Phys. J.* **C 58** (2008) 639 [arXiv:0803.0883] [INSPIRE].

[40] C.-Y. Wong and G. Wilk, *Tsallis fits to p_T spectra for pp collisions at LHC*, *Acta Phys. Polon.* **B 43** (2012) 2047 [arXiv:1210.3661] [INSPIRE].

[41] CMS collaboration, *Nuclear effects on the transverse momentum spectra of charged particles in p-Pb collisions at $\sqrt{s_{NN}} = 5.02$ TeV*, *Eur. Phys. J.* **C 75** (2015) 237 [arXiv:1502.05387] [INSPIRE].

[42] CMS collaboration, *CMS luminosity calibration for the pp reference run at $\sqrt{s} = 5.02$ TeV*, CMS-PAS-LUM-16-001 (2016).

[43] I. Helenius, K.J. Eskola, H. Honkanen and C.A. Salgado, *Impact-parameter dependent nuclear parton distribution functions: EPS09s and EKS98s and their applications in nuclear hard processes*, *JHEP* **07** (2012) 073 [arXiv:1205.5359] [INSPIRE].

[44] CMS collaboration, *Measurement of the elliptic anisotropy of charged particles produced in PbPb collisions at $\sqrt{s_{NN}} = 2.76$ TeV*, *Phys. Rev.* **C 87** (2013) 014902 [arXiv:1204.1409] [INSPIRE].

[45] PHENIX collaboration, A. Adare et al., *Spectra and ratios of identified particles in Au+Au and d+Au collisions at $\sqrt{s_{NN}} = 200$ GeV*, *Phys. Rev.* **C 88** (2013) 024906 [arXiv:1304.3410] [INSPIRE].

[46] C. Loizides and A. Morsch, *Absence of jet quenching in peripheral nucleus–nucleus collisions*, *Phys. Lett.* **B 773** (2017) 408 [arXiv:1705.08856] [INSPIRE].

[47] ALICE collaboration, *Analysis of the apparent nuclear modification in peripheral Pb-Pb collisions at 5.02 TeV*, arXiv:1805.05212 [INSPIRE].

[48] J. Jia, *Influence of the nucleon-nucleon collision geometry on the determination of the nuclear modification factor for nucleon-nucleus and nucleus-nucleus collisions*, *Phys. Lett.* **B 681** (2009) 320 [arXiv:0907.4175] [INSPIRE].

[49] Y. He, T. Luo, X.-N. Wang and Y. Zhu, *Linear Boltzmann transport for jet propagation in the quark-gluon plasma: elastic processes and medium recoil*, *Phys. Rev.* **C 91** (2015) 054908 [*Erratum ibid.* **C 97** (2018) 019902] [arXiv:1503.03313] [INSPIRE].

[50] S. Cao, T. Luo, G.-Y. Qin and X.-N. Wang, *Heavy and light flavor jet quenching at RHIC and LHC energies*, *Phys. Lett.* **B 777** (2018) 255 [arXiv:1703.00822] [INSPIRE].

[51] M. Djordjevic, *Theoretical formalism of radiative jet energy loss in a finite size dynamical QCD medium*, *Phys. Rev.* **C 80** (2009) 064909 [arXiv:0903.4591] [INSPIRE].

[52] M. Djordjevic and M. Djordjevic, *LHC jet suppression of light and heavy flavor observables*, *Phys. Lett.* **B 734** (2014) 286 [arXiv:1307.4098] [INSPIRE].

[53] J. Xu, J. Liao and M. Gyulassy, *Bridging soft-hard transport properties of quark-gluon plasmas with CUJET3.0*, *JHEP* **02** (2016) 169 [arXiv:1508.00552] [INSPIRE].

[54] S. Shi, J. Liao and M. Gyulassy, *Probing the color structure of the perfect QCD fluids via soft-hard-event-by-event azimuthal correlations*, *Chin. Phys.* **C 42** (2018) 104104 [arXiv:1804.01915] [INSPIRE].

[55] C. Andrés et al., *Energy versus centrality dependence of the jet quenching parameter $\hat{q}$ at RHIC and LHC: a new puzzle?*, *Eur. Phys. J.* **C 76** (2016) 475 [arXiv:1606.04837] [INSPIRE].

[56] Z.-B. Kang et al., *Jet quenching phenomenology from soft-collinear effective theory with Glauber gluons*, *Phys. Rev. Lett.* **114** (2015) 092002 [arXiv:1405.2612] [INSPIRE].

[57] Y.-T. Chien et al., *Jet quenching from QCD evolution*, *Phys. Rev.* **D 93** (2016) 074030 [arXiv:1509.02936] [INSPIRE].

The CMS collaboration

Yerevan Physics Institute, Yerevan, Armenia

A.M. Sirunyan, A. Tumasyan

Institut für Hochenergiephysik, Wien, Austria

W. Adam, F. Ambrogi, E. Asilar, T. Bergauer, J. Brandstetter, M. Dragicevic, J. Erö,
A. Escalante Del Valle, M. Flechl, R. Frühwirth[1], V.M. Ghete, J. Hrubec, M. Jeitler[1],
N. Krammer, I. Krätschmer, D. Liko, T. Madlener, I. Mikulec, N. Rad, H. Rohringer,
J. Schieck[1], R. Schöfbeck, M. Spanring, D. Spitzbart, A. Taurok, W. Waltenberger,
J. Wittmann, C.-E. Wulz[1], M. Zarucki

Institute for Nuclear Problems, Minsk, Belarus

V. Chekhovsky, V. Mossolov, J. Suarez Gonzalez

Universiteit Antwerpen, Antwerpen, Belgium

E.A. De Wolf, D. Di Croce, X. Janssen, J. Lauwers, M. Pieters, H. Van Haevermaet,
P. Van Mechelen, N. Van Remortel

Vrije Universiteit Brussel, Brussel, Belgium

S. Abu Zeid, F. Blekman, J. D'Hondt, I. De Bruyn, J. De Clercq, K. Deroover, G. Flouris,
D. Lontkovskyi, S. Lowette, I. Marchesini, S. Moortgat, L. Moreels, Q. Python, K. Skovpen,
S. Tavernier, W. Van Doninck, P. Van Mulders, I. Van Parijs

Université Libre de Bruxelles, Bruxelles, Belgium

D. Beghin, B. Bilin, H. Brun, B. Clerbaux, G. De Lentdecker, H. Delannoy, B. Dorney,
G. Fasanella, L. Favart, R. Goldouzian, A. Grebenyuk, A.K. Kalsi, T. Lenzi, J. Luetic,
N. Postiau, E. Starling, L. Thomas, C. Vander Velde, P. Vanlaer, D. Vannerom, Q. Wang

Ghent University, Ghent, Belgium

T. Cornelis, D. Dobur, A. Fagot, M. Gul, I. Khvastunov[2], D. Poyraz, C. Roskas, D. Trocino,
M. Tytgat, W. Verbeke, B. Vermassen, M. Vit, N. Zaganidis

Université Catholique de Louvain, Louvain-la-Neuve, Belgium

H. Bakhshiansohi, O. Bondu, S. Brochet, G. Bruno, C. Caputo, P. David, C. Delaere,
M. Delcourt, A. Giammanco, G. Krintiras, V. Lemaitre, A. Magitteri, A. Mertens,
M. Musich, K. Piotrzkowski, A. Saggio, M. Vidal Marono, S. Wertz, J. Zobec

Centro Brasileiro de Pesquisas Fisicas, Rio de Janeiro, Brazil

F.L. Alves, G.A. Alves, M. Correa Martins Junior, G. Correia Silva, C. Hensel, A. Moraes,
M.E. Pol, P. Rebello Teles

Universidade do Estado do Rio de Janeiro, Rio de Janeiro, Brazil

E. Belchior Batista Das Chagas, W. Carvalho, J. Chinellato[3], E. Coelho, E.M. Da Costa,
G.G. Da Silveira[4], D. De Jesus Damiao, C. De Oliveira Martins, S. Fonseca De Souza,
H. Malbouisson, D. Matos Figueiredo, M. Melo De Almeida, C. Mora Herrera, L. Mundim,
H. Nogima, W.L. Prado Da Silva, L.J. Sanchez Rosas, A. Santoro, A. Sznajder, M. Thiel,
E.J. Tonelli Manganote[3], F. Torres Da Silva De Araujo, A. Vilela Pereira

Universidade Estadual Paulista^a, Universidade Federal do ABC^b, São Paulo, Brazil

S. Ahuja^a, C.A. Bernardes^a, L. Calligaris^a, T.R. Fernandez Perez Tomei^a, E.M. Gregores^b, P.G. Mercadante^b, S.F. Novaes^a, SandraS. Padula^a

Institute for Nuclear Research and Nuclear Energy, Bulgarian Academy of Sciences, Sofia, Bulgaria

A. Aleksandrov, R. Hadjiiska, P. Iaydjiev, A. Marinov, M. Misheva, M. Rodozov, M. Shopova, G. Sultanov

University of Sofia, Sofia, Bulgaria

A. Dimitrov, L. Litov, B. Pavlov, P. Petkov

Beihang University, Beijing, China

W. Fang[5], X. Gao[5], L. Yuan

Institute of High Energy Physics, Beijing, China

M. Ahmad, J.G. Bian, G.M. Chen, H.S. Chen, M. Chen, Y. Chen, C.H. Jiang, D. Leggat, H. Liao, Z. Liu, F. Romeo, S.M. Shaheen[6], A. Spiezia, J. Tao, Z. Wang, E. Yazgan, H. Zhang, S. Zhang[6], J. Zhao

State Key Laboratory of Nuclear Physics and Technology, Peking University, Beijing, China

Y. Ban, G. Chen, A. Levin, J. Li, L. Li, Q. Li, Y. Mao, S.J. Qian, D. Wang, Z. Xu

Tsinghua University, Beijing, China

Y. Wang

Universidad de Los Andes, Bogota, Colombia

C. Avila, A. Cabrera, C.A. Carrillo Montoya, L.F. Chaparro Sierra, C. Florez, C.F. González Hernández, M.A. Segura Delgado

University of Split, Faculty of Electrical Engineering, Mechanical Engineering and Naval Architecture, Split, Croatia

B. Courbon, N. Godinovic, D. Lelas, I. Puljak, T. Sculac

University of Split, Faculty of Science, Split, Croatia

Z. Antunovic, M. Kovac

Institute Rudjer Boskovic, Zagreb, Croatia

V. Brigljevic, D. Ferencek, K. Kadija, B. Mesic, A. Starodumov[7], T. Susa

University of Cyprus, Nicosia, Cyprus

M.W. Ather, A. Attikis, M. Kolosova, G. Mavromanolakis, J. Mousa, C. Nicolaou, F. Ptochos, P.A. Razis, H. Rykaczewski

Charles University, Prague, Czech Republic

M. Finger[8], M. Finger Jr.[8]

Escuela Politecnica Nacional, Quito, Ecuador

E. Ayala

Universidad San Francisco de Quito, Quito, Ecuador

E. Carrera Jarrin

Academy of Scientific Research and Technology of the Arab Republic of Egypt, Egyptian Network of High Energy Physics, Cairo, Egypt

H. Abdalla[9], A.A. Abdelalim[10,11], M.A. Mahmoud[12,13]

National Institute of Chemical Physics and Biophysics, Tallinn, Estonia

S. Bhowmik, A. Carvalho Antunes De Oliveira, R.K. Dewanjee, K. Ehataht, M. Kadastik, M. Raidal, C. Veelken

Department of Physics, University of Helsinki, Helsinki, Finland

P. Eerola, H. Kirschenmann, J. Pekkanen, M. Voutilainen

Helsinki Institute of Physics, Helsinki, Finland

J. Havukainen, J.K. Heikkilä, T. Järvinen, V. Karimäki, R. Kinnunen, T. Lampén, K. Lassila-Perini, S. Laurila, S. Lehti, T. Lindén, P. Luukka, T. Mäenpää, H. Siikonen, E. Tuominen, J. Tuominiemi

Lappeenranta University of Technology, Lappeenranta, Finland

T. Tuuva

IRFU, CEA, Université Paris-Saclay, Gif-sur-Yvette, France

M. Besancon, F. Couderc, M. Dejardin, D. Denegri, J.L. Faure, F. Ferri, S. Ganjour, A. Givernaud, P. Gras, G. Hamel de Monchenault, P. Jarry, C. Leloup, E. Locci, J. Malcles, G. Negro, J. Rander, A. Rosowsky, M.Ö. Sahin, M. Titov

Laboratoire Leprince-Ringuet, Ecole polytechnique, CNRS/IN2P3, Université Paris-Saclay, Palaiseau, France

A. Abdulsalam[14], C. Amendola, I. Antropov, F. Beaudette, P. Busson, C. Charlot, R. Granier de Cassagnac, I. Kucher, A. Lobanov, J. Martin Blanco, C. Martin Perez, M. Nguyen, C. Ochando, G. Ortona, P. Pigard, J. Rembser, R. Salerno, J.B. Sauvan, Y. Sirois, A.G. Stahl Leiton, A. Zabi, A. Zghiche

Université de Strasbourg, CNRS, IPHC UMR 7178, F-67000 Strasbourg, France

J.-L. Agram[15], J. Andrea, D. Bloch, J.-M. Brom, E.C. Chabert, V. Cherepanov, C. Collard, E. Conte[15], J.-C. Fontaine[15], D. Gelé, U. Goerlach, M. Jansová, A.-C. Le Bihan, N. Tonon, P. Van Hove

Centre de Calcul de l'Institut National de Physique Nucleaire et de Physique des Particules, CNRS/IN2P3, Villeurbanne, France

S. Gadrat

Université de Lyon, Université Claude Bernard Lyon 1, CNRS-IN2P3, Institut de Physique Nucléaire de Lyon, Villeurbanne, France

S. Beauceron, C. Bernet, G. Boudoul, N. Chanon, R. Chierici, D. Contardo, P. Depasse, H. El Mamouni, J. Fay, L. Finco, S. Gascon, M. Gouzevitch, G. Grenier, B. Ille, F. Lagarde, I.B. Laktineh, H. Lattaud, M. Lethuillier, L. Mirabito, S. Perries, A. Popov[16], V. Sordini, G. Touquet, M. Vander Donckt, S. Viret

Georgian Technical University, Tbilisi, Georgia

T. Toriashvili[17]

Tbilisi State University, Tbilisi, Georgia

Z. Tsamalaidze[8]

RWTH Aachen University, I. Physikalisches Institut, Aachen, Germany

C. Autermann, L. Feld, M.K. Kiesel, K. Klein, M. Lipinski, M. Preuten, M.P. Rauch, C. Schomakers, J. Schulz, M. Teroerde, B. Wittmer, V. Zhukov[16]

RWTH Aachen University, III. Physikalisches Institut A, Aachen, Germany

A. Albert, D. Duchardt, M. Erdmann, S. Erdweg, T. Esch, R. Fischer, S. Ghosh, A. Güth, T. Hebbeker, C. Heidemann, K. Hoepfner, H. Keller, L. Mastrolorenzo, M. Merschmeyer, A. Meyer, P. Millet, S. Mukherjee, T. Pook, M. Radziej, H. Reithler, M. Rieger, A. Schmidt, D. Teyssier, S. Thüer

RWTH Aachen University, III. Physikalisches Institut B, Aachen, Germany

G. Flügge, O. Hlushchenko, T. Kress, A. Künsken, T. Müller, A. Nehrkorn, A. Nowack, C. Pistone, O. Pooth, D. Roy, H. Sert, A. Stahl[18]

Deutsches Elektronen-Synchrotron, Hamburg, Germany

M. Aldaya Martin, T. Arndt, C. Asawatangtrakuldee, I. Babounikau, K. Beernaert, O. Behnke, U. Behrens, A. Bermúdez Martínez, D. Bertsche, A.A. Bin Anuar, K. Borras[19], V. Botta, A. Campbell, P. Connor, C. Contreras-Campana, V. Danilov, A. De Wit, M.M. Defranchis, C. Diez Pardos, D. Domínguez Damiani, G. Eckerlin, T. Eichhorn, A. Elwood, E. Eren, E. Gallo[20], A. Geiser, A. Grohsjean, M. Guthoff, M. Haranko, A. Harb, J. Hauk, H. Jung, M. Kasemann, J. Keaveney, C. Kleinwort, J. Knolle, D. Krücker, W. Lange, A. Lelek, T. Lenz, J. Leonard, K. Lipka, W. Lohmann[21], R. Mankel, I.-A. Melzer-Pellmann, A.B. Meyer, M. Meyer, M. Missiroli, G. Mittag, J. Mnich, V. Myronenko, S.K. Pflitsch, D. Pitzl, A. Raspereza, M. Savitskyi, P. Saxena, P. Schütze, C. Schwanenberger, R. Shevchenko, A. Singh, H. Tholen, O. Turkot, A. Vagnerini, G.P. Van Onsem, R. Walsh, Y. Wen, K. Wichmann, C. Wissing, O. Zenaiev

University of Hamburg, Hamburg, Germany

R. Aggleton, S. Bein, L. Benato, A. Benecke, V. Blobel, T. Dreyer, A. Ebrahimi, E. Garutti, D. Gonzalez, P. Gunnellini, J. Haller, A. Hinzmann, A. Karavdina, G. Kasieczka, R. Klanner, R. Kogler, N. Kovalchuk, S. Kurz, V. Kutzner, J. Lange, D. Marconi, J. Multhaup, M. Niedziela, C.E.N. Niemeyer, D. Nowatschin, A. Perieanu, A. Reimers, O. Rieger, C. Scharf, P. Schleper, S. Schumann, J. Schwandt, J. Sonneveld, H. Stadie, G. Steinbrück, F.M. Stober, M. Stöver, A. Vanhoefer, B. Vormwald, I. Zoi

Karlsruher Institut fuer Technology

M. Akbiyik, C. Barth, M. Baselga, S. Baur, E. Butz, R. Caspart, T. Chwalek, F. Colombo, W. De Boer, A. Dierlamm, K. El Morabit, N. Faltermann, B. Freund, M. Giffels, M.A. Harrendorf, F. Hartmann[18], S.M. Heindl, U. Husemann, F. Kassel[18], I. Katkov[16], S. Kudella, S. Mitra, M.U. Mozer, Th. Müller, M. Plagge, G. Quast, K. Rabbertz, M. Schröder, I. Shvetsov, G. Sieber, H.J. Simonis, R. Ulrich, S. Wayand, M. Weber, T. Weiler, S. Williamson, C. Wöhrmann, R. Wolf

Institute of Nuclear and Particle Physics (INPP), NCSR Demokritos, Aghia Paraskevi, Greece

G. Anagnostou, G. Daskalakis, T. Geralis, A. Kyriakis, D. Loukas, G. Paspalaki, I. Topsis-Giotis

National and Kapodistrian University of Athens, Athens, Greece

B. Francois, G. Karathanasis, S. Kesisoglou, P. Kontaxakis, A. Panagiotou, I. Papavergou, N. Saoulidou, E. Tziaferi, K. Vellidis

National Technical University of Athens, Athens, Greece

K. Kousouris, I. Papakrivopoulos, G. Tsipolitis

University of Ioánnina, Ioánnina, Greece

I. Evangelou, C. Foudas, P. Gianneios, P. Katsoulis, P. Kokkas, S. Mallios, N. Manthos, I. Papadopoulos, E. Paradas, J. Strologas, F.A. Triantis, D. Tsitsonis

MTA-ELTE Lendület CMS Particle and Nuclear Physics Group, Eötvös Loránd University, Budapest, Hungary

M. Bartók[22], M. Csanad, N. Filipovic, P. Major, M.I. Nagy, G. Pasztor, O. Surányi, G.I. Veres

Wigner Research Centre for Physics, Budapest, Hungary

G. Bencze, C. Hajdu, D. Horvath[23], Á. Hunyadi, F. Sikler, T.Á. Vámi, V. Veszpremi, G. Vesztergombi[†]

Institute of Nuclear Research ATOMKI, Debrecen, Hungary

N. Beni, S. Czellar, J. Karancsi[24], A. Makovec, J. Molnar, Z. Szillasi

Institute of Physics, University of Debrecen, Debrecen, Hungary

P. Raics, Z.L. Trocsanyi, B. Ujvari

Indian Institute of Science (IISc), Bangalore, India

S. Choudhury, J.R. Komaragiri, P.C. Tiwari

National Institute of Science Education and Research, HBNI, Bhubaneswar, India

S. Bahinipati[25], C. Kar, P. Mal, K. Mandal, A. Nayak[26], D.K. Sahoo[25], S.K. Swain

Panjab University, Chandigarh, India

S. Bansal, S.B. Beri, V. Bhatnagar, S. Chauhan, R. Chawla, N. Dhingra, R. Gupta, A. Kaur, M. Kaur, S. Kaur, R. Kumar, P. Kumari, M. Lohan, A. Mehta, K. Sandeep, S. Sharma, J.B. Singh, A.K. Virdi, G. Walia

University of Delhi, Delhi, India

A. Bhardwaj, B.C. Choudhary, R.B. Garg, M. Gola, S. Keshri, Ashok Kumar, S. Malhotra, M. Naimuddin, P. Priyanka, K. Ranjan, Aashaq Shah, R. Sharma

Saha Institute of Nuclear Physics, HBNI, Kolkata, India

R. Bhardwaj[27], M. Bharti[27], R. Bhattacharya, S. Bhattacharya, U. Bhawandeep[27], D. Bhowmik, S. Dey, S. Dutt[27], S. Dutta, S. Ghosh, K. Mondal, S. Nandan, A. Purohit, P.K. Rout, A. Roy, S. Roy Chowdhury, G. Saha, S. Sarkar, M. Sharan, B. Singh[27], S. Thakur[27]

Indian Institute of Technology Madras, Madras, India

P.K. Behera

Bhabha Atomic Research Centre, Mumbai, India

R. Chudasama, D. Dutta, V. Jha, V. Kumar, P.K. Netrakanti, L.M. Pant, P. Shukla

Tata Institute of Fundamental Research-A, Mumbai, India

T. Aziz, M.A. Bhat, S. Dugad, G.B. Mohanty, N. Sur, B. Sutar, RavindraKumar Verma

Tata Institute of Fundamental Research-B, Mumbai, India

S. Banerjee, S. Bhattacharya, S. Chatterjee, P. Das, M. Guchait, Sa. Jain, S. Karmakar, S. Kumar, M. Maity[28], G. Majumder, K. Mazumdar, N. Sahoo, T. Sarkar[28]

Indian Institute of Science Education and Research (IISER), Pune, India

S. Chauhan, S. Dube, V. Hegde, A. Kapoor, K. Kothekar, S. Pandey, A. Rane, S. Sharma

Institute for Research in Fundamental Sciences (IPM), Tehran, Iran

S. Chenarani[29], E. Eskandari Tadavani, S.M. Etesami[29], M. Khakzad, M. Mohammadi Najafabadi, M. Naseri, F. Rezaei Hosseinabadi, B. Safarzadeh[30], M. Zeinali

University College Dublin, Dublin, Ireland

M. Felcini, M. Grunewald

INFN Sezione di Bari[a], Università di Bari[b], Politecnico di Bari[c], Bari, Italy

M. Abbrescia[a,b], C. Calabria[a,b], A. Colaleo[a], D. Creanza[a,c], L. Cristella[a,b], N. De Filippis[a,c], M. De Palma[a,b], A. Di Florio[a,b], F. Errico[a,b], L. Fiore[a], A. Gelmi[a,b], G. Iaselli[a,c], M. Ince[a,b], S. Lezki[a,b], G. Maggi[a,c], M. Maggi[a], G. Miniello[a,b], S. My[a,b], S. Nuzzo[a,b], A. Pompili[a,b], G. Pugliese[a,c], R. Radogna[a], A. Ranieri[a], G. Selvaggi[a,b], A. Sharma[a], L. Silvestris[a], R. Venditti[a], P. Verwilligen[a], G. Zito[a]

INFN Sezione di Bologna[a], Università di Bologna[b], Bologna, Italy

G. Abbiendi[a], C. Battilana[a,b], D. Bonacorsi[a,b], L. Borgonovi[a,b], S. Braibant-Giacomelli[a,b], R. Campanini[a,b], P. Capiluppi[a,b], A. Castro[a,b], F.R. Cavallo[a], S.S. Chhibra[a,b], C. Ciocca[a], G. Codispoti[a,b], M. Cuffiani[a,b], G.M. Dallavalle[a], F. Fabbri[a], A. Fanfani[a,b], E. Fontanesi,

P. Giacomelli[a], C. Grandi[a], L. Guiducci[a,b], F. Iemmi[a,b], S. Marcellini[a], G. Masetti[a], A. Montanari[a], F.L. Navarria[a,b], A. Perrotta[a], F. Primavera[a,b,18], A.M. Rossi[a,b], T. Rovelli[a,b], G.P. Siroli[a,b], N. Tosi[a]

INFN Sezione di Catania[a], Università di Catania[b], Catania, Italy

S. Albergo[a,b], A. Di Mattia[a], R. Potenza[a,b], A. Tricomi[a,b], C. Tuve[a,b]

INFN Sezione di Firenze[a], Università di Firenze[b], Firenze, Italy

G. Barbagli[a], K. Chatterjee[a,b], V. Ciulli[a,b], C. Civinini[a], R. D'Alessandro[a,b], E. Focardi[a,b], G. Latino, P. Lenzi[a,b], M. Meschini[a], S. Paoletti[a], L. Russo[a,31], G. Sguazzoni[a], D. Strom[a], L. Viliani[a]

INFN Laboratori Nazionali di Frascati, Frascati, Italy

L. Benussi, S. Bianco, F. Fabbri, D. Piccolo

INFN Sezione di Genova[a], Università di Genova[b], Genova, Italy

F. Ferro[a], F. Ravera[a,b], E. Robutti[a], S. Tosi[a,b]

INFN Sezione di Milano-Bicocca[a], Università di Milano-Bicocca[b], Milano, Italy

A. Benaglia[a], A. Beschi[b], L. Brianza[a,b], F. Brivio[a,b], V. Ciriolo[a,b,18], S. Di Guida[a,d,18], M.E. Dinardo[a,b], S. Fiorendi[a,b], S. Gennai[a], A. Ghezzi[a,b], P. Govoni[a,b], M. Malberti[a,b], S. Malvezzi[a], A. Massironi[a,b], D. Menasce[a], F. Monti, L. Moroni[a], M. Paganoni[a,b], D. Pedrini[a], S. Ragazzi[a,b], T. Tabarelli de Fatis[a,b], D. Zuolo[a,b]

INFN Sezione di Napoli[a], Università di Napoli 'Federico II'[b], Napoli, Italy, Università della Basilicata[c], Potenza, Italy, Università G. Marconi[d], Roma, Italy

S. Buontempo[a], N. Cavallo[a,c], A. De Iorio[a,b], A. Di Crescenzo[a,b], F. Fabozzi[a,c], F. Fienga[a], G. Galati[a], A.O.M. Iorio[a,b], W.A. Khan[a], L. Lista[a], S. Meola[a,d,18], P. Paolucci[a,18], C. Sciacca[a,b], E. Voevodina[a,b]

INFN Sezione di Padova[a], Università di Padova[b], Padova, Italy, Università di Trento[c], Trento, Italy

P. Azzi[a], N. Bacchetta[a], D. Bisello[a,b], A. Boletti[a,b], A. Bragagnolo, R. Carlin[a,b], P. Checchia[a], M. Dall'Osso[a,b], P. De Castro Manzano[a], T. Dorigo[a], U. Dosselli[a], F. Gasparini[a,b], U. Gasparini[a,b], A. Gozzelino[a], S.Y. Hoh, S. Lacaprara[a], P. Lujan, M. Margoni[a,b], A.T. Meneguzzo[a,b], J. Pazzini[a,b], P. Ronchese[a,b], R. Rossin[a,b], F. Simonetto[a,b], A. Tiko, E. Torassa[a], M. Zanetti[a,b], P. Zotto[a,b], G. Zumerle[a,b]

INFN Sezione di Pavia[a], Università di Pavia[b], Pavia, Italy

A. Braghieri[a], A. Magnani[a], P. Montagna[a,b], S.P. Ratti[a,b], V. Re[a], M. Ressegotti[a,b], C. Riccardi[a,b], P. Salvini[a], I. Vai[a,b], P. Vitulo[a,b]

INFN Sezione di Perugia[a], Università di Perugia[b], Perugia, Italy

M. Biasini[a,b], G.M. Bilei[a], C. Cecchi[a,b], D. Ciangottini[a,b], L. Fanò[a,b], P. Lariccia[a,b], R. Leonardi[a,b], E. Manoni[a], G. Mantovani[a,b], V. Mariani[a,b], M. Menichelli[a], A. Rossi[a,b], A. Santocchia[a,b], D. Spiga[a]

INFN Sezione di Pisa[a], Università di Pisa[b], Scuola Normale Superiore di Pisa[c], Pisa, Italy

K. Androsov[a], P. Azzurri[a], G. Bagliesi[a], L. Bianchini[a], T. Boccali[a], L. Borrello, R. Castaldi[a], M.A. Ciocci[a,b], R. Dell'Orso[a], G. Fedi[a], F. Fiori[a,c], L. Giannini[a,c], A. Giassi[a], M.T. Grippo[a], F. Ligabue[a,c], E. Manca[a,c], G. Mandorli[a,c], A. Messineo[a,b], F. Palla[a], A. Rizzi[a,b], P. Spagnolo[a], R. Tenchini[a], G. Tonelli[a,b], A. Venturi[a], P.G. Verdini[a]

INFN Sezione di Roma[a], Sapienza Università di Roma[b], Rome, Italy

L. Barone[a,b], F. Cavallari[a], M. Cipriani[a,b], D. Del Re[a,b], E. Di Marco[a,b], M. Diemoz[a], S. Gelli[a,b], E. Longo[a,b], B. Marzocchi[a,b], P. Meridiani[a], G. Organtini[a,b], F. Pandolfi[a], R. Paramatti[a,b], F. Preiato[a,b], S. Rahatlou[a,b], C. Rovelli[a], F. Santanastasio[a,b]

INFN Sezione di Torino[a], Università di Torino[b], Torino, Italy, Università del Piemonte Orientale[c], Novara, Italy

N. Amapane[a,b], R. Arcidiacono[a,c], S. Argiro[a,b], M. Arneodo[a,c], N. Bartosik[a], R. Bellan[a,b], C. Biino[a], N. Cartiglia[a], F. Cenna[a,b], S. Cometti[a], M. Costa[a,b], R. Covarelli[a,b], N. Demaria[a], B. Kiani[a,b], C. Mariotti[a], S. Maselli[a], E. Migliore[a,b], V. Monaco[a,b], E. Monteil[a,b], M. Monteno[a], M.M. Obertino[a,b], L. Pacher[a,b], N. Pastrone[a], M. Pelliccioni[a], G.L. Pinna Angioni[a,b], A. Romero[a,b], M. Ruspa[a,c], R. Sacchi[a,b], K. Shchelina[a,b], V. Sola[a], A. Solano[a,b], D. Soldi[a,b], A. Staiano[a]

INFN Sezione di Trieste[a], Università di Trieste[b], Trieste, Italy

S. Belforte[a], V. Candelise[a,b], M. Casarsa[a], F. Cossutti[a], A. Da Rold[a,b], G. Della Ricca[a,b], F. Vazzoler[a,b], A. Zanetti[a]

Kyungpook National University

D.H. Kim, G.N. Kim, M.S. Kim, J. Lee, S. Lee, S.W. Lee, C.S. Moon, Y.D. Oh, S.I. Pak, S. Sekmen, D.C. Son, Y.C. Yang

Chonnam National University, Institute for Universe and Elementary Particles, Kwangju, Korea

H. Kim, D.H. Moon, G. Oh

Hanyang University, Seoul, Korea

J. Goh[32], T.J. Kim

Korea University, Seoul, Korea

S. Cho, S. Choi, Y. Go, D. Gyun, S. Ha, B. Hong, Y. Jo, K. Lee, K.S. Lee, S. Lee, J. Lim, S.K. Park, Y. Roh

Sejong University, Seoul, Korea

H.S. Kim

Seoul National University, Seoul, Korea

J. Almond, J. Kim, J.S. Kim, H. Lee, K. Lee, K. Nam, S.B. Oh, B.C. Radburn-Smith, S.h. Seo, U.K. Yang, H.D. Yoo, G.B. Yu

University of Seoul, Seoul, Korea

D. Jeon, H. Kim, J.H. Kim, J.S.H. Lee, I.C. Park

Sungkyunkwan University, Suwon, Korea

Y. Choi, C. Hwang, J. Lee, I. Yu

Vilnius University, Vilnius, Lithuania

V. Dudenas, A. Juodagalvis, J. Vaitkus

National Centre for Particle Physics, Universiti Malaya, Kuala Lumpur, Malaysia

I. Ahmed, Z.A. Ibrahim, M.A.B. Md Ali[33], F. Mohamad Idris[34], W.A.T. Wan Abdullah, M.N. Yusli, Z. Zolkapli

Universidad de Sonora (UNISON), Hermosillo, Mexico

J.F. Benitez, A. Castaneda Hernandez, J.A. Murillo Quijada

Centro de Investigacion y de Estudios Avanzados del IPN, Mexico City, Mexico

H. Castilla-Valdez, E. De La Cruz-Burelo, M.C. Duran-Osuna, I. Heredia-De La Cruz[35], R. Lopez-Fernandez, J. Mejia Guisao, R.I. Rabadan-Trejo, M. Ramirez-Garcia, G. Ramirez-Sanchez, R Reyes-Almanza, A. Sanchez-Hernandez

Universidad Iberoamericana, Mexico City, Mexico

S. Carrillo Moreno, C. Oropeza Barrera, F. Vazquez Valencia

Benemerita Universidad Autonoma de Puebla, Puebla, Mexico

J. Eysermans, I. Pedraza, H.A. Salazar Ibarguen, C. Uribe Estrada

Universidad Autónoma de San Luis Potosí, San Luis Potosí, Mexico

A. Morelos Pineda

University of Auckland, Auckland, New Zealand

D. Krofcheck

University of Canterbury, Christchurch, New Zealand

S. Bheesette, P.H. Butler

National Centre for Physics, Quaid-I-Azam University, Islamabad, Pakistan

A. Ahmad, M. Ahmad, M.I. Asghar, Q. Hassan, H.R. Hoorani, A. Saddique, M.A. Shah, M. Shoaib, M. Waqas

National Centre for Nuclear Research, Swierk, Poland

H. Bialkowska, M. Bluj, B. Boimska, T. Frueboes, M. Górski, M. Kazana, M. Szleper, P. Traczyk, P. Zalewski

Institute of Experimental Physics, Faculty of Physics, University of Warsaw, Warsaw, Poland

K. Bunkowski, A. Byszuk[36], K. Doroba, A. Kalinowski, M. Konecki, J. Krolikowski, M. Misiura, M. Olszewski, A. Pyskir, M. Walczak

Laboratório de Instrumentação e Física Experimental de Partículas, Lisboa, Portugal

M. Araujo, P. Bargassa, C. Beirão Da Cruz E Silva, A. Di Francesco, P. Faccioli, B. Galinhas, M. Gallinaro, J. Hollar, N. Leonardo, M.V. Nemallapudi, J. Seixas, G. Strong, O. Toldaiev, D. Vadruccio, J. Varela

Joint Institute for Nuclear Research, Dubna, Russia

S. Afanasiev, P. Bunin, M. Gavrilenko, I. Golutvin, I. Gorbunov, A. Kamenev, V. Karjavine, A. Lanev, A. Malakhov, V. Matveev[37,38], P. Moisenz, V. Palichik, V. Perelygin, S. Shmatov, S. Shulha, N. Skatchkov, V. Smirnov, N. Voytishin, A. Zarubin

Petersburg Nuclear Physics Institute, Gatchina (St. Petersburg), Russia

V. Golovtsov, Y. Ivanov, V. Kim[39], E. Kuznetsova[40], P. Levchenko, V. Murzin, V. Oreshkin, I. Smirnov, D. Sosnov, V. Sulimov, L. Uvarov, S. Vavilov, A. Vorobyev

Institute for Nuclear Research, Moscow, Russia

Yu. Andreev, A. Dermenev, S. Gninenko, N. Golubev, A. Karneyeu, M. Kirsanov, N. Krasnikov, A. Pashenkov, D. Tlisov, A. Toropin

Institute for Theoretical and Experimental Physics, Moscow, Russia

V. Epshteyn, V. Gavrilov, N. Lychkovskaya, V. Popov, I. Pozdnyakov, G. Safronov, A. Spiridonov, A. Stepennov, V. Stolin, M. Toms, E. Vlasov, A. Zhokin

Moscow Institute of Physics and Technology, Moscow, Russia

T. Aushev

National Research Nuclear University 'Moscow Engineering Physics Institute' (MEPhI), Moscow, Russia

R. Chistov[41], P. Parygin, D. Philippov, S. Polikarpov[41], E. Popova, E. Tarkovskii

P.N. Lebedev Physical Institute, Moscow, Russia

V. Andreev, M. Azarkin, I. Dremin[38], M. Kirakosyan, S.V. Rusakov, A. Terkulov

Skobeltsyn Institute of Nuclear Physics, Lomonosov Moscow State University, Moscow, Russia

A. Baskakov, A. Belyaev, E. Boos, A. Ershov, A. Gribushin, A. Kaminskiy[42], O. Kodolova, V. Korotkikh, I. Lokhtin, I. Miagkov, S. Obraztsov, S. Petrushanko, V. Savrin, A. Snigirev, I. Vardanyan

Novosibirsk State University (NSU), Novosibirsk, Russia

A. Barnyakov[43], V. Blinov[43], T. Dimova[43], L. Kardapoltsev[43], Y. Skovpen[43]

State Research Center of Russian Federation, Institute for High Energy Physics of NRC 'Kurchatov Institute', Protvino, Russia

I. Azhgirey, I. Bayshev, S. Bitioukov, D. Elumakhov, A. Godizov, V. Kachanov, A. Kalinin, D. Konstantinov, P. Mandrik, V. Petrov, R. Ryutin, S. Slabospitskii, A. Sobol, S. Troshin, N. Tyurin, A. Uzunian, A. Volkov

National Research Tomsk Polytechnic University, Tomsk, Russia

A. Babaev, S. Baidali, V. Okhotnikov

University of Belgrade, Faculty of Physics and Vinca Institute of Nuclear Sciences, Belgrade, Serbia

P. Adzic[44], P. Cirkovic, D. Devetak, M. Dordevic, J. Milosevic

Centro de Investigaciones Energéticas Medioambientales y Tecnológicas (CIEMAT), Madrid, Spain

J. Alcaraz Maestre, A. Álvarez Fernández, I. Bachiller, M. Barrio Luna, J.A. Brochero Cifuentes, M. Cerrada, N. Colino, B. De La Cruz, A. Delgado Peris, C. Fernandez Bedoya, J.P. Fernández Ramos, J. Flix, M.C. Fouz, O. Gonzalez Lopez, S. Goy Lopez, J.M. Hernandez, M.I. Josa, D. Moran, A. Pérez-Calero Yzquierdo, J. Puerta Pelayo, I. Redondo, L. Romero, M.S. Soares, A. Triossi

Universidad Autónoma de Madrid, Madrid, Spain

C. Albajar, J.F. de Trocóniz

Universidad de Oviedo, Oviedo, Spain

J. Cuevas, C. Erice, J. Fernandez Menendez, S. Folgueras, I. Gonzalez Caballero, J.R. González Fernández, E. Palencia Cortezon, V. Rodríguez Bouza, S. Sanchez Cruz, P. Vischia, J.M. Vizan Garcia

Instituto de Física de Cantabria (IFCA), CSIC-Universidad de Cantabria, Santander, Spain

I.J. Cabrillo, A. Calderon, B. Chazin Quero, J. Duarte Campderros, M. Fernandez, P.J. Fernández Manteca, A. García Alonso, J. Garcia-Ferrero, G. Gomez, A. Lopez Virto, J. Marco, C. Martinez Rivero, P. Martinez Ruiz del Arbol, F. Matorras, J. Piedra Gomez, C. Prieels, T. Rodrigo, A. Ruiz-Jimeno, L. Scodellaro, N. Trevisani, I. Vila, R. Vilar Cortabitarte

University of Ruhuna, Department of Physics, Matara, Sri Lanka

N. Wickramage

CERN, European Organization for Nuclear Research, Geneva, Switzerland

D. Abbaneo, B. Akgun, E. Auffray, G. Auzinger, P. Baillon, A.H. Ball, D. Barney, J. Bendavid, M. Bianco, A. Bocci, C. Botta, E. Brondolin, T. Camporesi, M. Cepeda, G. Cerminara, E. Chapon, Y. Chen, G. Cucciati, D. d'Enterria, A. Dabrowski, N. Daci, V. Daponte, A. David, A. De Roeck, N. Deelen, M. Dobson, M. Dünser, N. Dupont, A. Elliott-Peisert, P. Everaerts, F. Fallavollita[45], D. Fasanella, G. Franzoni, J. Fulcher, W. Funk, D. Gigi, A. Gilbert, K. Gill, F. Glege, M. Guilbaud, D. Gulhan, J. Hegeman, C. Heidegger, V. Innocente, A. Jafari, P. Janot, O. Karacheban[21], J. Kieseler, A. Kornmayer, M. Krammer[1], C. Lange, P. Lecoq, C. Lourenço, L. Malgeri, M. Mannelli, F. Meijers, J.A. Merlin, S. Mersi, E. Meschi, P. Milenovic[46], F. Moortgat, M. Mulders, J. Ngadiuba, S. Nourbakhsh, S. Orfanelli, L. Orsini, F. Pantaleo[18], L. Pape, E. Perez, M. Peruzzi, A. Petrilli, G. Petrucciani, A. Pfeiffer, M. Pierini, F.M. Pitters, D. Rabady, A. Racz, T. Reis, G. Rolandi[47], M. Rovere, H. Sakulin, C. Schäfer, C. Schwick, M. Seidel,

M. Selvaggi, A. Sharma, P. Silva, P. Sphicas[48], A. Stakia, J. Steggemann, M. Tosi, D. Treille, A. Tsirou, V. Veckalns[49], M. Verzetti, W.D. Zeuner

Paul Scherrer Institut, Villigen, Switzerland

L. Caminada[50], K. Deiters, W. Erdmann, R. Horisberger, Q. Ingram, H.C. Kaestli, D. Kotlinski, U. Langenegger, T. Rohe, S.A. Wiederkehr

ETH Zurich — Institute for Particle Physics and Astrophysics (IPA), Zurich, Switzerland

M. Backhaus, L. Bäni, P. Berger, N. Chernyavskaya, G. Dissertori, M. Dittmar, M. Donegà, C. Dorfer, T.A. Gómez Espinosa, C. Grab, D. Hits, T. Klijnsma, W. Lustermann, R.A. Manzoni, M. Marionneau, M.T. Meinhard, F. Micheli, P. Musella, F. Nessi-Tedaldi, J. Pata, F. Pauss, G. Perrin, L. Perrozzi, S. Pigazzini, M. Quittnat, C. Reissel, D. Ruini, D.A. Sanz Becerra, M. Schönenberger, L. Shchutska, V.R. Tavolaro, K. Theofilatos, M.L. Vesterbacka Olsson, R. Wallny, D.H. Zhu

Universität Zürich, Zurich, Switzerland

T.K. Aarrestad, C. Amsler[51], D. Brzhechko, M.F. Canelli, A. De Cosa, R. Del Burgo, S. Donato, C. Galloni, T. Hreus, B. Kilminster, S. Leontsinis, I. Neutelings, G. Rauco, P. Robmann, D. Salerno, K. Schweiger, C. Seitz, Y. Takahashi, A. Zucchetta

National Central University, Chung-Li, Taiwan

Y.H. Chang, K.y. Cheng, T.H. Doan, R. Khurana, C.M. Kuo, W. Lin, A. Pozdnyakov, S.S. Yu

National Taiwan University (NTU), Taipei, Taiwan

P. Chang, Y. Chao, K.F. Chen, P.H. Chen, W.-S. Hou, Arun Kumar, Y.F. Liu, R.-S. Lu, E. Paganis, A. Psallidas, A. Steen

Chulalongkorn University, Faculty of Science, Department of Physics, Bangkok, Thailand

B. Asavapibhop, N. Srimanobhas, N. Suwonjandee

Çukurova University, Physics Department, Science and Art Faculty, Adana, Turkey

A. Bat, F. Boran, S. Cerci[52], S. Damarseckin, Z.S. Demiroglu, F. Dolek, C. Dozen, I. Dumanoglu, S. Girgis, G. Gokbulut, Y. Guler, E. Gurpinar, I. Hos[53], C. Isik, E.E. Kangal[54], O. Kara, A. Kayis Topaksu, U. Kiminsu, M. Oglakci, G. Onengut, K. Ozdemir[55], S. Ozturk[56], D. Sunar Cerci[52], B. Tali[52], U.G. Tok, S. Turkcapar, I.S. Zorbakir, C. Zorbilmez

Middle East Technical University, Physics Department, Ankara, Turkey

B. Isildak[57], G. Karapinar[58], M. Yalvac, M. Zeyrek

Bogazici University, Istanbul, Turkey

I.O. Atakisi, E. Gülmez, M. Kaya[59], O. Kaya[60], S. Tekten, E.A. Yetkin[61]

Istanbul Technical University, Istanbul, Turkey

M.N. Agaras, A. Cakir, K. Cankocak, Y. Komurcu, S. Sen[62]

Institute for Scintillation Materials of National Academy of Science of Ukraine, Kharkov, Ukraine

B. Grynyov

National Scientific Center, Kharkov Institute of Physics and Technology, Kharkov, Ukraine

L. Levchuk

University of Bristol, Bristol, United Kingdom

F. Ball, L. Beck, J.J. Brooke, D. Burns, E. Clement, D. Cussans, O. Davignon, H. Flacher, J. Goldstein, G.P. Heath, H.F. Heath, L. Kreczko, D.M. Newbold[63], S. Paramesvaran, B. Penning, T. Sakuma, D. Smith, V.J. Smith, J. Taylor, A. Titterton

Rutherford Appleton Laboratory, Didcot, United Kingdom

A. Belyaev[64], C. Brew, R.M. Brown, D. Cieri, D.J.A. Cockerill, J.A. Coughlan, K. Harder, S. Harper, J. Linacre, E. Olaiya, D. Petyt, C.H. Shepherd-Themistocleous, A. Thea, I.R. Tomalin, T. Williams, W.J. Womersley

Imperial College, London, United Kingdom

R. Bainbridge, P. Bloch, J. Borg, S. Breeze, O. Buchmuller, A. Bundock, D. Colling, P. Dauncey, G. Davies, M. Della Negra, R. Di Maria, Y. Haddad, G. Hall, G. Iles, T. James, M. Komm, C. Laner, L. Lyons, A.-M. Magnan, S. Malik, A. Martelli, J. Nash[65], A. Nikitenko[7], V. Palladino, M. Pesaresi, D.M. Raymond, A. Richards, A. Rose, E. Scott, C. Seez, A. Shtipliyski, G. Singh, M. Stoye, T. Strebler, S. Summers, A. Tapper, K. Uchida, T. Virdee[18], N. Wardle, D. Winterbottom, J. Wright, S.C. Zenz

Brunel University, Uxbridge, United Kingdom

J.E. Cole, P.R. Hobson, A. Khan, P. Kyberd, C.K. Mackay, A. Morton, I.D. Reid, L. Teodorescu, S. Zahid

Baylor University, Waco, U.S.A.

K. Call, J. Dittmann, K. Hatakeyama, H. Liu, C. Madrid, B. Mcmaster, N. Pastika, C. Smith

Catholic University of America, Washington DC, U.S.A.

R. Bartek, A. Dominguez

The University of Alabama, Tuscaloosa, U.S.A.

A. Buccilli, S.I. Cooper, C. Henderson, P. Rumerio, C. West

Boston University, Boston, U.S.A.

D. Arcaro, T. Bose, D. Gastler, D. Pinna, D. Rankin, C. Richardson, J. Rohlf, L. Sulak, D. Zou

Brown University, Providence, U.S.A.

G. Benelli, X. Coubez, D. Cutts, M. Hadley, J. Hakala, U. Heintz, J.M. Hogan[66], K.H.M. Kwok, E. Laird, G. Landsberg, J. Lee, Z. Mao, M. Narain, S. Sagir[67], R. Syarif, E. Usai, D. Yu

University of California, Davis, Davis, U.S.A.

R. Band, C. Brainerd, R. Breedon, D. Burns, M. Calderon De La Barca Sanchez, M. Chertok, J. Conway, R. Conway, P.T. Cox, R. Erbacher, C. Flores, G. Funk, W. Ko, O. Kukral, R. Lander, M. Mulhearn, D. Pellett, J. Pilot, S. Shalhout, M. Shi, D. Stolp, D. Taylor, K. Tos, M. Tripathi, Z. Wang, F. Zhang

University of California, Los Angeles, U.S.A.

M. Bachtis, C. Bravo, R. Cousins, A. Dasgupta, A. Florent, J. Hauser, M. Ignatenko, N. Mccoll, S. Regnard, D. Saltzberg, C. Schnaible, V. Valuev

University of California, Riverside, Riverside, U.S.A.

E. Bouvier, K. Burt, R. Clare, J.W. Gary, S.M.A. Ghiasi Shirazi, G. Hanson, G. Karapostoli, E. Kennedy, F. Lacroix, O.R. Long, M. Olmedo Negrete, M.I. Paneva, W. Si, L. Wang, H. Wei, S. Wimpenny, B.R. Yates

University of California, San Diego, La Jolla, U.S.A.

J.G. Branson, P. Chang, S. Cittolin, M. Derdzinski, R. Gerosa, D. Gilbert, B. Hashemi, A. Holzner, D. Klein, G. Kole, V. Krutelyov, J. Letts, M. Masciovecchio, D. Olivito, S. Padhi, M. Pieri, M. Sani, V. Sharma, S. Simon, M. Tadel, A. Vartak, S. Wasserbaech[68], J. Wood, F. Würthwein, A. Yagil, G. Zevi Della Porta

University of California, Santa Barbara — Department of Physics, Santa Barbara, U.S.A.

N. Amin, R. Bhandari, J. Bradmiller-Feld, C. Campagnari, M. Citron, A. Dishaw, V. Dutta, M. Franco Sevilla, L. Gouskos, R. Heller, J. Incandela, A. Ovcharova, H. Qu, J. Richman, D. Stuart, I. Suarez, S. Wang, J. Yoo

California Institute of Technology, Pasadena, U.S.A.

D. Anderson, A. Bornheim, J.M. Lawhorn, H.B. Newman, T.Q. Nguyen, M. Spiropulu, J.R. Vlimant, R. Wilkinson, S. Xie, Z. Zhang, R.Y. Zhu

Carnegie Mellon University, Pittsburgh, U.S.A.

M.B. Andrews, T. Ferguson, T. Mudholkar, M. Paulini, M. Sun, I. Vorobiev, M. Weinberg

University of Colorado Boulder, Boulder, U.S.A.

J.P. Cumalat, W.T. Ford, F. Jensen, A. Johnson, M. Krohn, E. MacDonald, T. Mulholland, R. Patel, A. Perloff, K. Stenson, K.A. Ulmer, S.R. Wagner

Cornell University, Ithaca, U.S.A.

J. Alexander, J. Chaves, Y. Cheng, J. Chu, A. Datta, K. Mcdermott, N. Mirman, J.R. Patterson, D. Quach, A. Rinkevicius, A. Ryd, L. Skinnari, L. Soffi, S.M. Tan, Z. Tao, J. Thom, J. Tucker, P. Wittich, M. Zientek

Fermi National Accelerator Laboratory, Batavia, U.S.A.

S. Abdullin, M. Albrow, M. Alyari, G. Apollinari, A. Apresyan, A. Apyan, S. Banerjee, L.A.T. Bauerdick, A. Beretvas, J. Berryhill, P.C. Bhat, K. Burkett, J.N. Butler, A. Canepa, G.B. Cerati, H.W.K. Cheung, F. Chlebana, M. Cremonesi, J. Duarte, V.D. Elvira, J. Freeman, Z. Gecse, E. Gottschalk, L. Gray, D. Green, S. Grünendahl, O. Gutsche,

J. Hanlon, R.M. Harris, S. Hasegawa, J. Hirschauer, Z. Hu, B. Jayatilaka, S. Jindariani, M. Johnson, U. Joshi, B. Klima, M.J. Kortelainen, B. Kreis, S. Lammel, D. Lincoln, R. Lipton, M. Liu, T. Liu, J. Lykken, K. Maeshima, J.M. Marraffino, D. Mason, P. McBride, P. Merkel, S. Mrenna, S. Nahn, V. O'Dell, K. Pedro, C. Pena, O. Prokofyev, G. Rakness, L. Ristori, A. Savoy-Navarro[69], B. Schneider, E. Sexton-Kennedy, A. Soha, W.J. Spalding, L. Spiegel, S. Stoynev, J. Strait, N. Strobbe, L. Taylor, S. Tkaczyk, N.V. Tran, L. Uplegger, E.W. Vaandering, C. Vernieri, M. Verzocchi, R. Vidal, M. Wang, H.A. Weber, A. Whitbeck

University of Florida, Gainesville, U.S.A.

D. Acosta, P. Avery, P. Bortignon, D. Bourilkov, A. Brinkerhoff, L. Cadamuro, A. Carnes, M. Carver, D. Curry, R.D. Field, S.V. Gleyzer, B.M. Joshi, J. Konigsberg, A. Korytov, K.H. Lo, P. Ma, K. Matchev, H. Mei, G. Mitselmakher, D. Rosenzweig, K. Shi, D. Sperka, J. Wang, S. Wang, X. Zuo

Florida International University, Miami, U.S.A.

Y.R. Joshi, S. Linn

Florida State University, Tallahassee, U.S.A.

A. Ackert, T. Adams, A. Askew, S. Hagopian, V. Hagopian, K.F. Johnson, T. Kolberg, G. Martinez, T. Perry, H. Prosper, A. Saha, C. Schiber, R. Yohay

Florida Institute of Technology, Melbourne, U.S.A.

M.M. Baarmand, V. Bhopatkar, S. Colafranceschi, M. Hohlmann, D. Noonan, M. Rahmani, T. Roy, F. Yumiceva

University of Illinois at Chicago (UIC), Chicago, U.S.A.

M.R. Adams, L. Apanasevich, D. Berry, R.R. Betts, R. Cavanaugh, X. Chen, S. Dittmer, O. Evdokimov, C.E. Gerber, D.A. Hangal, D.J. Hofman, K. Jung, J. Kamin, C. Mills, I.D. Sandoval Gonzalez, M.B. Tonjes, H. Trauger, N. Varelas, H. Wang, X. Wang, Z. Wu, J. Zhang

The University of Iowa, Iowa City, U.S.A.

M. Alhusseini, B. Bilki[70], W. Clarida, K. Dilsiz[71], S. Durgut, R.P. Gandrajula, M. Haytmyradov, V. Khristenko, J.-P. Merlo, A. Mestvirishvili, A. Moeller, J. Nachtman, H. Ogul[72], Y. Onel, F. Ozok[73], A. Penzo, C. Snyder, E. Tiras, J. Wetzel

Johns Hopkins University, Baltimore, U.S.A.

B. Blumenfeld, A. Cocoros, N. Eminizer, D. Fehling, L. Feng, A.V. Gritsan, W.T. Hung, P. Maksimovic, J. Roskes, U. Sarica, M. Swartz, M. Xiao, C. You

The University of Kansas, Lawrence, U.S.A.

A. Al-bataineh, P. Baringer, A. Bean, S. Boren, J. Bowen, A. Bylinkin, J. Castle, S. Khalil, A. Kropivnitskaya, D. Majumder, W. Mcbrayer, M. Murray, C. Rogan, S. Sanders, E. Schmitz, J.D. Tapia Takaki, Q. Wang

Kansas State University, Manhattan, U.S.A.

S. Duric, A. Ivanov, K. Kaadze, D. Kim, Y. Maravin, D.R. Mendis, T. Mitchell, A. Modak, A. Mohammadi, L.K. Saini, N. Skhirtladze

Lawrence Livermore National Laboratory, Livermore, U.S.A.

F. Rebassoo, D. Wright

University of Maryland, College Park, U.S.A.

A. Baden, O. Baron, A. Belloni, S.C. Eno, Y. Feng, C. Ferraioli, N.J. Hadley, S. Jabeen, G.Y. Jeng, R.G. Kellogg, J. Kunkle, A.C. Mignerey, S. Nabili, F. Ricci-Tam, Y.H. Shin, A. Skuja, S.C. Tonwar, K. Wong

Massachusetts Institute of Technology, Cambridge, U.S.A.

D. Abercrombie, B. Allen, V. Azzolini, A. Baty, G. Bauer, R. Bi, S. Brandt, W. Busza, I.A. Cali, M. D'Alfonso, Z. Demiragli, G. Gomez Ceballos, M. Goncharov, P. Harris, D. Hsu, M. Hu, Y. Iiyama, G.M. Innocenti, M. Klute, D. Kovalskyi, Y.-J. Lee, P.D. Luckey, B. Maier, A.C. Marini, C. Mcginn, C. Mironov, S. Narayanan, X. Niu, C. Paus, C. Roland, G. Roland, G.S.F. Stephans, K. Sumorok, K. Tatar, D. Velicanu, J. Wang, T.W. Wang, B. Wyslouch, S. Zhaozhong

University of Minnesota, Minneapolis, U.S.A.

A.C. Benvenuti[†], R.M. Chatterjee, A. Evans, P. Hansen, Sh. Jain, S. Kalafut, Y. Kubota, Z. Lesko, J. Mans, N. Ruckstuhl, R. Rusack, J. Turkewitz, M.A. Wadud

University of Mississippi, Oxford, U.S.A.

J.G. Acosta, S. Oliveros

University of Nebraska-Lincoln, Lincoln, U.S.A.

E. Avdeeva, K. Bloom, D.R. Claes, C. Fangmeier, F. Golf, R. Gonzalez Suarez, R. Kamalieddin, I. Kravchenko, J. Monroy, J.E. Siado, G.R. Snow, B. Stieger

State University of New York at Buffalo, Buffalo, U.S.A.

A. Godshalk, C. Harrington, I. Iashvili, A. Kharchilava, C. Mclean, D. Nguyen, A. Parker, S. Rappoccio, B. Roozbahani

Northeastern University, Boston, U.S.A.

G. Alverson, E. Barberis, C. Freer, A. Hortiangtham, D.M. Morse, T. Orimoto, R. Teixeira De Lima, T. Wamorkar, B. Wang, A. Wisecarver, D. Wood

Northwestern University, Evanston, U.S.A.

S. Bhattacharya, O. Charaf, K.A. Hahn, N. Mucia, N. Odell, M.H. Schmitt, K. Sung, M. Trovato, M. Velasco

University of Notre Dame, Notre Dame, U.S.A.

R. Bucci, N. Dev, M. Hildreth, K. Hurtado Anampa, C. Jessop, D.J. Karmgard, N. Kellams, K. Lannon, W. Li, N. Loukas, N. Marinelli, F. Meng, C. Mueller, Y. Musienko[37], M. Planer, A. Reinsvold, R. Ruchti, P. Siddireddy, G. Smith, S. Taroni, M. Wayne, A. Wightman, M. Wolf, A. Woodard

The Ohio State University, Columbus, U.S.A.

J. Alimena, L. Antonelli, B. Bylsma, L.S. Durkin, S. Flowers, B. Francis, A. Hart, C. Hill, W. Ji, T.Y. Ling, W. Luo, B.L. Winer

Princeton University, Princeton, U.S.A.

S. Cooperstein, P. Elmer, J. Hardenbrook, S. Higginbotham, A. Kalogeropoulos, D. Lange, M.T. Lucchini, J. Luo, D. Marlow, K. Mei, I. Ojalvo, J. Olsen, C. Palmer, P. Piroué, J. Salfeld-Nebgen, D. Stickland, C. Tully

University of Puerto Rico, Mayaguez, U.S.A.

S. Malik, S. Norberg

Purdue University, West Lafayette, U.S.A.

A. Barker, V.E. Barnes, S. Das, L. Gutay, M. Jones, A.W. Jung, A. Khatiwada, B. Mahakud, D.H. Miller, N. Neumeister, C.C. Peng, S. Piperov, H. Qiu, J.F. Schulte, J. Sun, F. Wang, R. Xiao, W. Xie

Purdue University Northwest, Hammond, U.S.A.

T. Cheng, J. Dolen, N. Parashar

Rice University, Houston, U.S.A.

Z. Chen, K.M. Ecklund, S. Freed, F.J.M. Geurts, M. Kilpatrick, W. Li, B.P. Padley, R. Redjimi, J. Roberts, J. Rorie, W. Shi, Z. Tu, J. Zabel, A. Zhang

University of Rochester, Rochester, U.S.A.

A. Bodek, P. de Barbaro, R. Demina, Y.t. Duh, J.L. Dulemba, C. Fallon, T. Ferbel, M. Galanti, A. Garcia-Bellido, J. Han, O. Hindrichs, A. Khukhunaishvili, P. Tan, R. Taus

Rutgers, The State University of New Jersey, Piscataway, U.S.A.

A. Agapitos, J.P. Chou, Y. Gershtein, E. Halkiadakis, M. Heindl, E. Hughes, S. Kaplan, R. Kunnawalkam Elayavalli, S. Kyriacou, A. Lath, R. Montalvo, K. Nash, M. Osherson, H. Saka, S. Salur, S. Schnetzer, D. Sheffield, S. Somalwar, R. Stone, S. Thomas, P. Thomassen, M. Walker

University of Tennessee, Knoxville, U.S.A.

A.G. Delannoy, J. Heideman, G. Riley, S. Spanier

Texas A&M University, College Station, U.S.A.

O. Bouhali[74], A. Celik, M. Dalchenko, M. De Mattia, A. Delgado, S. Dildick, R. Eusebi, J. Gilmore, T. Huang, T. Kamon[75], S. Luo, R. Mueller, D. Overton, L. Perniè, D. Rathjens, A. Safonov

Texas Tech University, Lubbock, U.S.A.

N. Akchurin, J. Damgov, F. De Guio, P.R. Dudero, S. Kunori, K. Lamichhane, S.W. Lee, T. Mengke, S. Muthumuni, T. Peltola, S. Undleeb, I. Volobouev, Z. Wang

Vanderbilt University, Nashville, U.S.A.

S. Greene, A. Gurrola, R. Janjam, W. Johns, C. Maguire, A. Melo, H. Ni, K. Padeken, J.D. Ruiz Alvarez, P. Sheldon, S. Tuo, J. Velkovska, M. Verweij, Q. Xu

University of Virginia, Charlottesville, U.S.A.

M.W. Arenton, P. Barria, B. Cox, R. Hirosky, M. Joyce, A. Ledovskoy, H. Li, C. Neu, T. Sinthuprasith, Y. Wang, E. Wolfe, F. Xia

Wayne State University, Detroit, U.S.A.

R. Harr, P.E. Karchin, N. Poudyal, J. Sturdy, P. Thapa, S. Zaleski

University of Wisconsin — Madison, Madison, WI, U.S.A.

M. Brodski, J. Buchanan, C. Caillol, D. Carlsmith, S. Dasu, L. Dodd, B. Gomber, M. Grothe, M. Herndon, A. Hervé, U. Hussain, P. Klabbers, A. Lanaro, K. Long, R. Loveless, T. Ruggles, A. Savin, V. Sharma, N. Smith, W.H. Smith, N. Woods

37: Also at Institute for Nuclear Research, Moscow, Russia

38: Now at National Research Nuclear University 'Moscow Engineering Physics Institute' (MEPhI), Moscow, Russia

39: Also at St. Petersburg State Polytechnical University, St. Petersburg, Russia

40: Also at University of Florida, Gainesville, U.S.A.

41: Also at P.N. Lebedev Physical Institute, Moscow, Russia

42: Also at INFN Sezione di Padova^a, Università di Padova^b, Università di Trento (Trento)^c, Padova, Italy

43: Also at Budker Institute of Nuclear Physics, Novosibirsk, Russia

44: Also at Faculty of Physics, University of Belgrade, Belgrade, Serbia

45: Also at INFN Sezione di Pavia^a, Università di Pavia^b, Pavia, Italy

46: Also at University of Belgrade, Faculty of Physics and Vinca Institute of Nuclear Sciences, Belgrade, Serbia

47: Also at Scuola Normale e Sezione dell'INFN, Pisa, Italy

48: Also at National and Kapodistrian University of Athens, Athens, Greece

49: Also at Riga Technical University, Riga, Latvia

50: Also at Universität Zürich, Zurich, Switzerland

51: Also at Stefan Meyer Institute for Subatomic Physics (SMI), Vienna, Austria

52: Also at Adiyaman University, Adiyaman, Turkey

53: Also at Istanbul Aydin University, Istanbul, Turkey

54: Also at Mersin University, Mersin, Turkey

55: Also at Piri Reis University, Istanbul, Turkey

56: Also at Gaziosmanpasa University, Tokat, Turkey

57: Also at Ozyegin University, Istanbul, Turkey

58: Also at Izmir Institute of Technology, Izmir, Turkey

59: Also at Marmara University, Istanbul, Turkey

60: Also at Kafkas University, Kars, Turkey

61: Also at Istanbul Bilgi University, Istanbul, Turkey

62: Also at Hacettepe University, Ankara, Turkey

63: Also at Rutherford Appleton Laboratory, Didcot, United Kingdom

64: Also at School of Physics and Astronomy, University of Southampton, Southampton, United Kingdom

65: Also at Monash University, Faculty of Science, Clayton, Australia

66: Also at Bethel University, St. Paul, U.S.A.

67: Also at Karamanoğlu Mehmetbey University, Karaman, Turkey

68: Also at Utah Valley University, Orem, U.S.A.

69: Also at Purdue University, West Lafayette, U.S.A.

70: Also at Beykent University, Istanbul, Turkey

71: Also at Bingol University, Bingol, Turkey

72: Also at Sinop University, Sinop, Turkey

73: Also at Mimar Sinan University, Istanbul, Istanbul, Turkey

74: Also at Texas A&M University at Qatar, Doha, Qatar

75: Also at Kyungpook National University, Daegu, Korea